



<https://theses.gla.ac.uk/>

Theses Digitisation:

<https://www.gla.ac.uk/myglasgow/research/enlighten/theses/digitisation/>

This is a digitised version of the original print thesis.

Copyright and moral rights for this work are retained by the author

A copy can be downloaded for personal non-commercial research or study,
without prior permission or charge

This work cannot be reproduced or quoted extensively from without first
obtaining permission in writing from the author

The content must not be changed in any way or sold commercially in any
format or medium without the formal permission of the author

When referring to this work, full bibliographic details including the author,
title, awarding institution and date of the thesis must be given

Enlighten: Theses

<https://theses.gla.ac.uk/>
research-enlighten@glasgow.ac.uk

EFFECT OF FLEXIBLE BEDS ON FLOW STABILITY

IN OPEN CHANNELS

by

A.M. Hatata

University of Glasgow

Department of Aeronautics and Fluid Mechanics

February 1964

ProQuest Number: 10662755

All rights reserved

INFORMATION TO ALL USERS

The quality of this reproduction is dependent upon the quality of the copy submitted.

In the unlikely event that the author did not send a complete manuscript and there are missing pages, these will be noted. Also, if material had to be removed, a note will indicate the deletion.



ProQuest 10662755

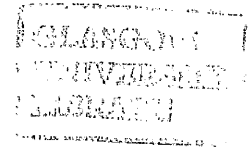
Published by ProQuest LLC (2017). Copyright of the Dissertation is held by the Author.

All rights reserved.

This work is protected against unauthorized copying under Title 17, United States Code
Microform Edition © ProQuest LLC.

ProQuest LLC.
789 East Eisenhower Parkway
P.O. Box 1346
Ann Arbor, MI 48106 – 1346

"SUMMARY"



A brief review is given of the available theoretical and experimental work of Nonweiler and Kramer relating to the effect of surface flexibility on the maintenance of laminar flow in water.

This thesis describes the results of tests on a sample of a thin sheet of soft rubber used as a bed for an open channel. The influence of this flexible bed on the stability of flow in open channels is discussed with special reference to the effect of delaying transition from laminar to turbulent flow. To this end, two criteria analogous to those of Nonweiler - the one for the elimination of the Tollmien-Schlichting waves, and the other for the elimination of the flexural waves - are applied to the consideration of the effects of possible changes in the bed material (to melinex for example).

Transition was inferred from measurements of the friction coefficient and Reynolds number. The experimental procedure for measuring the friction coefficient and Reynolds number is discussed, and also the experimental limitations which affected the measurements (hydraulic jump, and unevenness of the

rubber bed for example).

Owing to the limitations of accuracy, a statistical analysis for the results had to be applied in order to find the most probable values of Reynolds number for transition. It was found that if the 90% probability level is considered, the flow is likely to be laminar at a value of Reynolds number of about 620, transitional at a value of Reynolds number between 1600 and 1800, and turbulent at a value of Reynolds number equal to 2370.

It seemed doubtful whether the flexible bed used, maintained the laminar flow, when compared with rigid beds having the same shape. The material used for the bed may be thought, perhaps, to be so thin that flexural waves exist; this seemed to be indicated by gross instabilities observed in the flow when the bed was tensioned enough to ensure that the whole width of the channel was wetted.

Other flexible materials are suggested which are thought probably to have better stabilizing effect on the flow.

GLASGOW
UNIVERSITY

Thesis
2386
Copy 2

GLASGOW
UNIVERSITY
LIBRARY

CONTENTS

	Page
1. Introduction	1
2. Choice, properties and testing of the bed material.	8
2.1. Choice of the bed material.	8
2.2. Properties of the elastic material.	15
2.3. Testing of the rubber.	16
3. Description of the apparatus and methods of measurements.	19
3.1. The apparatus.	19
3.2. Methods of measurements.	20
3.2.1. First method of measurement.	20
3.2.2. Second method of measurement.	21
3.3. Shape of rubber deformed by water pressure.	25
3.4. Method of interpolation.	28
4. Free surface slope, coefficient of friction and Reynolds number for steady channel flow.	29
4.1. Free surface slope.	29
4.2. Coefficient of friction and Reynolds number.	32
4.2.1. Laminar flow.	34
4.2.2. Turbulent flow.	34
5. Observations and Results.	36
5.1. Observations.	36
5.1.a. Hydraulic jump.	36
5.1.b. Unevenness of the glass bed.	37
5.1.c. Unevenness of the rubber bed.	38
5.4. Results.	38
6. Tests with the rubber bed being tightened.	39

7.	Statistical analysis and conclusions.	40
7.1.	Statistical analysis.	40
7.2.	Conclusions.	44
8.	Appendices.	
I.	Development of a method for measuring the ordinates at specially selected points.	47
II.	Shape of rubber deformed by water pressure.	53
III.	Corrections for the area, depth of flow and wetted perimeter.	60
IV.	Method of interpolation.	63
V.	Free surface slope and probable errors.	68
VI.	Coefficient of friction for steady channel flow.	71
VII.	Statistical analysis.	74

Tables.

Figures.

ACKNOWLEDGEMENT

This thesis was submitted on application for the degree of M.Sc. (Eng.) The work was carried out in the Department of Aeronautics and Fluids Mechanics in the Engineering Faculty of Glasgow University.

The author would like to express his appreciation to Professor T.R.F. Nonweiler for his interest and assistance throughout this research. He is also grateful to Dr. A.S. Thom and Mr. H. Wong for their assistance during the course of the work.

1.

INTRODUCTION

A series of papers by Kramer (1,2,3) has appeared in which he describes experiments conducted mainly on a torpedo-shaped body towed under water. It is claimed that appreciable drag reductions were found in certain conditions, and that this was due to the damping distributed over the flexible surface which stabilized the flow and resulted in an increased extent of laminar boundary layer. This mechanism of boundary layer control was suggested to Kramer by his microscopic studies of the structure of the skin of a dolphin,⁽⁴⁾ whose outstanding top speed performance suggests that the drag coefficient of the animal in these conditions must have a value appropriate to wholly laminar flow.

Kramer's tests showed that over the whole speed range of the tests the drag coefficient when the torpedo-shaped body was fitted with flexible surfaces was always less than when the surface was rigid.

Skins of varying stiffnesses were tested, each over a range of values of the viscosity of the damping fluid. The best results at top speed were obtained with a coating of stiffness 800lb/sq.inch/inch when filled

with damping fluid 300 centistokes. The drag was then 59 per cent of that of the rigid surface model, which implies 83 per cent laminar flow, or a five times increase in transition Reynolds number.

Similar problems are theoretically treated by Nonweiler,⁽⁵⁾ where he developed an appropriate form of the boundary layer stability equation for the condition where the fluid is in contact with an isotropic and homogeneous elastic medium, and obtained various approximate analytical solutions for certain types of surface, so as to reveal qualitatively the origin and characteristics of neutral oscillations. In the worked solution the elastic medium is treated as non-dissipative, and the interior boundary is supposed either fixed, or free of stress, or exposed to fluid, the boundary layer, in addition, is treated as that over a flat plate in an incompressible fluid.

The purpose of the work described in this thesis is to investigate the stability of open channel flow over a flexible bed, which is clamped along side supports parallel to the flow direction, so as to support the fluid by tension alone. In endeavouring to examine this work in relation to that of Kramer, it is of course at once evident that the value of Reynolds number for

transition is not the same for flow in channels as that for a flow past a plate. The boundary layer becomes turbulent for flow past a semi-infinite plate at

$$R_x = \frac{Ux}{\nu} \approx 3 \times 10^5$$

where x is the distance from the forward point and ν is the kinematic viscosity, or at

$$R_\delta = \frac{U\delta}{\nu} \approx 1000$$

when evaluated with respect to the thickness δ of the boundary layer. The value of Reynolds number of transition for flow in open channels is

$$R = \frac{vm}{\nu} \approx 500,$$

where v is the mean velocity of flow and m is the hydraulic mean depth.

There is also a difference between the flexible material used for the channel bed and that used by Kramer. The bed material used consisted of a thin elastic sheeting of rubber 0.023" thick, clamped along the side supports of a channel, while that of Kramer was a heavy rubber diaphragm 0.08" thick, supported by a multitude of tiny rubber stubs representing a multitude of capillary ducts which could be filled with a damping fluid of appropriate viscosity.

However, Nonweiler suggests in his theory two

interesting criteria for the stability of the boundary layer in contact with a flexible skin, and an analogy to these criteria will be used in this present investigation. His first criterion is that for the elimination of Tollmien Schlichting waves (small regular oscillations in the laminar boundary layer which grow up when the boundary layer becomes turbulent), we must make $(\theta^3 c_4^2 / \sigma u_\delta^2)$ less than in round numbers - say, 2000, where θ is the ratio of the thickness of the elastic skin to $\frac{u_\delta}{k}$,

k is the surface velocity gradient of the boundary layer,

c_4 is the speed of longitudinal waves in an extensive thin plate,

σ is the fluid density/elastic medium density, and u_δ is the free stream speed.

He predicted that c_p must be bigger than u_δ , as a second criterion for the elimination of the flexural mode. Then the minimum speed of propagation of the flexural mode has to be c_p where,

$$\left(\frac{c_p}{u_\delta}\right)^3 \approx 0.42 \left(\frac{\theta^3 c_4^2}{\sigma u_\delta^2}\right)^{\frac{1}{3}} \left(\frac{c_4}{u_\delta}\right)^{\frac{4}{3}} \frac{\sigma^{\frac{1}{3}}}{12 + \sigma}$$

this is of course approximate, as a simple criterion

however, this value of c_p (which is also inversely proportional to the largest wave length of amplified disturbances) may yet have some relevance to the extent of amplification.

Clearly, to make c_p large, we must take $(\theta^3 c_4^2 / \omega u_0^2)$ as close to its permissible upper bound (of 2000) as possible, and make u_0 / c_4 as small as possible, and not merely just less than unity.

However, these two criteria are not of course applicable to the present investigation. An analogy can perhaps be made for channel flow by forming similar non-dimensional groups relating the elastic properties of the material to some variables describing the flow. These two criteria analogous to those of Nonweiler would then be

$$\frac{Gt^3}{\frac{1}{2}\rho v^2 m^3} < N_1 \quad \text{for the elimination of the}$$

Tollmien-Schlichting waves

$$\frac{Gt}{\frac{1}{2}\rho v^2 m} > N_2 \quad \text{for the elimination of the}$$

flexural waves

where G is the modulus of rigidity of the elastic material in lb/ft.^2

t is the thickness of the material in ft.

-10-

ρ is the fluid density in $\frac{\text{lb. sec.}^2}{\text{ft.}^4}$

v is the mean velocity of flow in ft/sec.

m is the hydraulic mean depth in ft., and

N_1, N_2 are constants, the values of which are not yet determined.

However, Section 2 in this thesis is concerned with the choice of the elastic material of the bed, and contains a discussion concerning the effect of its elastic properties on the two criteria mentioned above, as well as a study of their effect on the behaviour of this material as a membrane (it will indeed be shown that the material of the bed we choose does behave like a membrane). The properties of the material of the bed, and the results of testing it under tension to find the modulus of elongation are also discussed in Section 2. In Section 3, a description of the channel and the methods of measurements are given, of which there are two: the results from the second method only are used since it gave better accuracy. In Section 4, the methods of calculating the free surface slope, coefficient of friction and Reynolds number for steady channel flow are given. The experimental results and observation are given in Section 5. In Section 6, there is a brief note about other tests conducted with the flexible bed tensioned

to ensure that the whole width of the channel was wetted. A statistical analysis is given in Section 7 to find what the most probable values of Reynolds number for laminar, transition and turbulent flows are likely to be, and the conclusions will also be found in this section.

2. CHOICE, PROPERTIES, AND TESTING OF THE BED MATERIAL

2.1 CHOICE OF BED MATERIAL

Considering Nonweiler's criteria, for the elimination of the Tollmien-Schlichting waves

$$\frac{\theta^3 c_4^2}{\sigma u_\delta^2} < 2000 \quad \text{i.e.} \quad \theta < \frac{2000}{c_4^2 \theta^2 / \sigma u_\delta^2} \dots\dots\dots (2.1.1.)$$

and for the elimination of the flexural waves

$$\left(\frac{c_p}{u_\delta}\right)^3 \approx 0.42 \left(\frac{\theta^3 c_4^2}{\sigma u_\delta^2}\right)^{\frac{1}{3}} \left(\frac{c_4}{u_\delta}\right)^{\frac{4}{3}} \frac{\sigma^{\frac{1}{3}}}{12 + \sigma}$$

if we put $\frac{c_p}{u_\delta}$, say, equal to unity and $\sigma = 1$, it

follows that

$$\frac{\theta c_4^2}{\sigma u_\delta^2} > \frac{12 + \sigma}{0.42 \sigma} \quad \text{i.e.} \quad \theta < \frac{1}{30} \frac{\theta^2 c_4^2}{\sigma u_\delta^2} \dots\dots\dots (2.1.2.)$$

If we draw the graphs of $\theta = \frac{2000}{x}$ and $\theta = \frac{x}{30}$ where $x = \frac{c_4^2 \theta^2}{\sigma u_\delta^2}$, these two graphs will

intersect at $x \approx 250$.

Therefore $\theta_{critical}$, which indicates the maximum allowable thickness, where no waves of either kind exist will be approximately 8. (see fig. 1).

The two analogous criteria for channel flow are given by

$$\frac{G t}{\frac{1}{2}\rho v^2 m} > N_1 \quad \text{for the elimination of the flexural waves} \dots\dots\dots (2.1.3.)$$

and $\frac{G t^3}{\frac{1}{2}\rho v^2 m^3} < N_2$ for the elimination of the Tollmien-Schlichting waves. $\dots\dots\dots (2.1.4.)$

Arranging both criteria together, we have

$$\frac{t}{m} < \frac{N_2}{\frac{G t^2}{\frac{1}{2}\rho v^2 m^2}} \quad , \quad \frac{G t^2}{N_1 \frac{1}{2}\rho v^2 m^2} \dots\dots\dots (2.1.5.)$$

Now, $\frac{t}{m}$ is analogous to θ in Nonweiler's criteria and $\frac{G t^2}{\frac{1}{2}\rho v^2 m^2}$, is analogous to $\frac{c_4^2 \theta^3}{u_\delta^2 \sigma}$,

therefore as before we can write

$$\frac{t}{m} < \frac{N_2}{x} < \frac{x}{N_1}$$

If we draw graphs of $\frac{t}{m} = \frac{N_2}{x}$ and $\frac{t}{m} = \frac{x}{N_1}$, this will allow us to find the region where the flexural waves and the Tollmien-Schlichting waves are present and where they are absent (see Fig. 1).

As an example, if we consider a value of v of about 1 ft./sec., and a value of m of about 0.06 ft.,

the value of $\frac{1}{2}\rho v^2 m^2$, will be approximately 35×10^{-4} lb. Let us consider some elastic materials of the same thickness say 0.02", but of different moduli of rigidity. The value of $\frac{Gt^2}{\frac{1}{2}\rho v^2 m^2}$, will be about 3 for soft rubber sheeting having a modulus of rigidity of about 30 p.s.i., on the other hand dealing with "Melinex" which have a modulus of rigidity of about 2×10^5 p.s.i., the value of $\frac{Gt^2}{\frac{1}{2}\rho v^2 m^2}$, will be about 23×10^3 .

If there is any relevance of Nonweiler's criteria for the stability of the boundary layer in contact with a flexible skin, to those criteria for the stability of flow in open channels, then we would guess a value of $\frac{250}{3}$ i.e., about 83 times G considered if the soft rubber is used, and a value of $\frac{250}{23 \times 10^3}$, i.e., about $\frac{1}{100}$ times G if "Melinex" is used. Referring to (Fig. 1) it may be clear that by increasing G, the corresponding value of $\frac{c_4}{u_\delta}$ will decrease, and will perhaps place the material in the region where the flexural waves exist. On the other hand, decreasing G will increase $\frac{c_4}{u_\delta}$, which will place the material where the Tollmien-Schlichting waves exist. Clearly there is no material with a modulus of rigidity less than that of soft rubber, so that such a reduction in G has practical limits. It will also be interesting to find the condition

that the material used for the bed should behave like a membrane when subjected to hydro-static pressure. For this condition to be fulfilled, the bending moment due to the weight of water on the bed must be much less than the horizontal component of the tension in the material times the distance where the moments are taken. Now, by taking moments about O (See Fig. 2), it follows that

$$T_h \cdot L + M = Wx$$

and the criteria will be satisfied, if

$$M \ll T_h \cdot L \quad \dots\dots\dots (2.1.6.)$$

where M is the bending moment

$$= EIK = \sigma GIK \quad \dots\dots\dots (2.1.7.)$$

E, G are the Young's modulus and modulus of rigidity respectively, I is the sectional moment of inertia of the skin = $\frac{t^3}{12}$ per unit span,

σ is Poisson ratio,

K is the curvature $\approx \frac{\theta}{w}$,

where θ is the inclination of the tangent plane to the rubber to the horizontal,

w is the wetted perimeter

T_h is the horizontal component of the tension,
 $= T_v \cot\theta$, where T_v is the vertical component of the tension = ρgA (2.1.8.)

ρ is the density of water

and A is the cross sectional area of flow.

Therefore if we substitute (2.1.7.), (2.1.8.) in (2.1.6.), it follows that Gt^3 must be very small compared with $\rho gAwL$ i.e.,

$$Gt^3 \ll \rho gAwL \dots\dots\dots (2.1.9.)$$

In the table below, we give a comparison between different materials to find the suitable thickness which satisfies the criteria (2.1.9.), assuming that Gt^3 must be less than or equal to 0.001, say, times $\rho gAwL$. We will consider a value of ρgA of , say, 2 lb/ft., a value of the wetted perimeter of, say, 0.5 ft., and a value of L about 0.3 ft., the product $\rho gAwL$, will be then 0.3 lb/ft., and Gt^3 must be about 3×10^{-4} lb/ft., or less.

MATERIAL	E	σ	G	t
Melinex	5×10^5	0.38	2×10^5	0.002 or less
Aluminium Foil	10×10^6	0.38	38×10^5	0.001 or less
Soft Rubber	10^2	0.33	33	0.05 or less
Strong Rubber	12×10^4	0.33	4×10^4	0.01 or less

where E is Young's Modulus (p.s.i.)

$\sigma = \frac{G}{E}$ is Poisson Ratio

G is Modulus of Rigidity (p.s.i.)

t (inches) is thickness of the material which satisfies the criterion of the behaviour like a membrane.

The materials compared are "Melinex" polyester film (which is the I.C.I., trade name for polyester film made from polyethylene terephthalate, the same raw material as used for the manufacture of "Terylene" fibres), aluminium foil, soft and strong vulcanized rubber. Any of these materials with their values for the modulus of rigidity and their values for the thickness as mentioned above in the table will satisfy the criterion (2.1.9.) for the behaviour of the material like a membrane.

Now any of these materials which will satisfy also the two criteria for the elimination of Tollmien-Schlichting waves and the flexural waves can be chosen for the present investigation. With "Melinex" the value of $\frac{Gt^2}{\frac{1}{2}\rho v^2 m^2}$ will be about 230 which is about 92 per cent of that of the critical value of (250), with Aluminium Foils this value is 1080 which is about 430 per cent of the critical value, with soft rubbers, the value is 23.6 which is about 9.4 per cent, and with strong rubbers the value is 1140, which is about 456 per cent of that of the

critical value. It seems therefore that the aluminium foil and the strong rubber will not be considered at all, since they do not satisfy the criteria for the elimination of the Tollmien-Schlichting waves and the flexural waves. It seems also that "Melinex" is the most suitable material and the soft rubber comes after it in preference.

When we thought about choosing the material, it seemed doubtful whether there was any likely relevance between Nonweiler's criterion for stabilizing the boundary layer, and those criteria for stabilizing the flow in open channels.

Merely because it was easily available, a sheet of soft vulcanized rubber, 0.023" thick was used for our investigation, and now that the experiments are complete it appears that such material is to be placed on the borders of the region where the flexural waves exist.

2.2

PROPERTIES OF THE ELASTIC MATERIAL

The material used for the channel bed was a thin sheeting of soft vulcanized rubber (rubber thread 505 count 6011 quality). This rubber was supplied by Dunlop Rubber Company.

With soft rubbers elongation of about 1000 per cent ⁽⁶⁾ (greater than those possible with ordinary solids by a factor of 10^5) are obtainable with relatively small deviations from complete reversibility. The stress-strain curves have an unusual S - form, the Young's modulus at first decreasing with increasing strain until it is of the order of about one third its value for small strains, and thereafter increasing more and more rapidly. The modulus of rigidity (G) ⁽⁷⁾, is equal to $\frac{E}{3}$. (This simple relation between the shear modulus and Young's modulus holds only if the polymer remains at a constant volume during the deformation, i.e., can be considered as "incompressible". This will be true for all soft polymers).

2.3

TESTING OF THE RUBBER

A piece of soft vulcanized rubber of length = 20" breadth = 1" and thickness = 0.023", was tested under tension by clamping it between two pairs of aluminium angles as shown in (Fig. 3). Weights were suspended from the lower pair of angles. A vertical scale was used for measuring the extension in the rubber corresponding to each load. The stresses were calculated for each loading based on the original cross sectional area of the tested piece. The strains were also calculated for each loading. The results obtained are tabulated in Table 1, and the relation between stress and strain is represented in Fig. 4.a, from which it is found that for very small percentages of elongation the stress is nearly proportional to strain or in other words the relation between the stretching force and the extension obeys Hook's law.

The experimental stress/strain curve may be compared with the manufacturer's (Dunlop Rubber Company) curve (Fig. 4b), and it is found that they are both nearly identical for a range up to 70 per cent elongation.

It is now important to discover in which range of the stress/strain curve the rubber extends under the

pressure of water. This is found by calculating the stress in the material due to the edge tension per unit length in the rubber.

The vertical component of the edge tension per unit length can be inferred as

$$v = \frac{\rho g Q}{T_v}, \quad \text{if the channel slope is small}$$

where v is the mean velocity flow and T_v is the vertical component of edge tension. The resultant tension in the material is

$$T = \frac{T_v}{\sin \theta} \quad (\text{where } \theta \text{ is the inclination of the tangent plane to the rubber bed to the horizontal}).$$

Therefore

$$T = \frac{\rho g A}{\sin \theta}$$

If $\rho g A$ is given the value 2 lb/ft., say and θ is 45° , say, then

$$T = 2.88 \text{ lb/ft.}$$

Considering the stress in the rubber at one side only, the stress per unit length is equal to

$$\frac{T}{2A_2} = \frac{2.88 \times 12}{2 \times 0.023} = 750 \text{ lb/ft.}^3$$

where A is the area of the cross section of the rubber

Therefore stress = 5.21 p.s.i.

This value of the stress corresponds to 5.21 per cent elongation and the value of Young's modulus will be approximately 100 p.s.i., which corresponds to a value of the modulus of rigidity (G) of 33.3 p.s.i.

3. DESCRIPTION OF THE APPARATUS AND METHODS OF MEASUREMENTS

3.1

THE APPARATUS

The apparatus consists of a pump unit, 20 foot flow channel with glass bed and sides, collecting tank 6 ft x 3 ft x 1 ft 6 in., and a base tank 18 ft x 3 ft x 1 ft 9 in., all connected in a closed circuit. The collecting tank is fixed on a weighing machine (reading up to 2500 lb.) at the down-stream end of the channel.

The channel is mounted on a truss supported at two points, one being a fixed point and the other a jack.

After removing the glass sides of the channel the rubber bed was clamped on to the two parallel angles supporting the channel. The rubber bed acted as a thin elastic surface exposed to fluid above, and unsupported below, and so the fluid was supported by the tension in the rubber bed (Fig. 5).

The slope of the channel was altered as required by means of the jack. At the upstream end a formed spillway rested on the original bed of the channel, and the rubber bed was sandwiched between the spillway and the modelling clay which covered the spillway. The clay was painted with a waterproof paint so as to prevent the direct contact of water with the clay. This was done to enable smooth entry

of the flow to the rubber bed and to minimize the entry losses (Fig. 6).

3.2 METHODS OF MEASUREMENTS

Two methods of measurements were used to obtain the variables describing the flow, each method will be described individually below.

3.2.1 FIRST METHOD OF MEASUREMENT

(a) The discharge Q was measured by collecting a certain quantity of water (1000 lbs.) in the collecting tank, the time " t " taken for collecting this amount was measured by means of an electric stop timer measuring to within $\frac{1}{10}$ of a second.

(b) The width of the free surface was measured by exposing the water surface to a lighting source, so as to make the two end lines of the free surface clearly observable by looking underneath the rubber bed (Fig. 7).

A micrometer height gauge which measures vertical ordinates to 0.001 of an inch (Fig. 8) was designed for the purpose of measuring the water profile. The micrometer slides on a 12 inch scale fixed at the section where the measurements have to be taken. By means of the index mark on the base of the micrometer the two end points (a,c) of the free surface were projected on the 12" scale. By reading the distances corresponding to (a,c) on the scale and subtracting (a) from (c), the width ($b = c - a$) was obtained.

(c) In the first set of experiments, the vertical ordinates of the profile were measured by the micrometer at equal distances apart of one inch. The first and last ordinates were measured outside the free surface of the rubber just for the sake of completing the profile.

The two ordinates at the end points (a,c) were not recorded but were obtained by graphical interpolation.

All the ordinates read were plotted full scale, and a planimeter was used for measuring the areas of flow at the different sections (Fig. 9).

(d) The depth of flow "h" was measured from the drawing at section 6" which was close to the point of maximum depth. An ordinary scale divided to $\frac{1}{10}$ of an inch was used for this measurement.

(e) In the first set of experiments, the wetted perimeter "W" was measured by means of a map measurer.

(f) The slope of the glass bed "S", was measured by closing the down-stream end by a gate, pumping a quantity of water to the channel and leaving it for a few minutes until the surface of the water settled. Thereafter two measurements of the depth of water at different points were taken by means of a pointer with a vernier carried on a travelling carriage and moving on the two rails mounted on the angles supporting the channel.

Errors arose from the graphical construction of the

profiles and the measurements made from them. By the method first described, these would be present in the area, the depth of flow and the wetted perimeter.

The method of measuring the slope was not practical because replacing and removing the glass sides proved too laborious.

None of the results based on this method of measurement are given in the thesis. The following method of measurement proved to be more acceptable.

3.2.2 SECOND METHOD OF MEASUREMENT

The discharge and the width of the free surface were measured by the method described in (3.2.1.).

The following measurements were, however, taken in a different way.

(a) In subsequent sets of experiments, the ordinates, including those at the end points were measured at a specially selected set of points, to suit a numerical quadrature formulae. The numerical quadrature formula used was one described by Professor T.R.F. Nonweiler, see (appendix I) as

$$\int_a^c f(x) dx = (c - a) \left\{ 0.02381 [f(x_1) + f(x_7)] + 0.13841 [f(x_2) + f(x_6)] + 0.21586 [f(x_3) + f(x_5)] + 0.24384 [f(x_4)] \right\} \dots (3.2.2.1)$$

where

$$\begin{aligned}
x_1 &= a \\
x_2 &= a + 0.08489(c - a) \\
x_3 &= a + 0.26557(c - a) \\
x_4 &= a + 0.5(c - a) \\
x_5 &= a + 0.73442(c - a) \\
x_6 &= a + 0.91511(c - a) \\
x_7 &= a + (c - a) = C
\end{aligned}$$

Evidently (a,c) in the present context are the end points of the free surface,

$$f(x_1) = \bar{y} - y_1, \quad f(x_2) = \bar{y} - y_2 \quad \dots\dots$$

where

$$\bar{y} = \frac{y_1 + y_7}{2}$$

and $y_1, y_2 \dots\dots$ are the measured ordinates.

This method reduced the errors inherent in the graphical method, and simplified the evaluation of the areas.

(b) The depth of flow (h) at the lowest point of the rubber bed is

$$(\bar{y} - y_4) = f(x_4)$$

All the values of $f(x_1), f(x_2), \dots\dots$ are tabulated in (Table 2), and the values of A, b and h are tabulated in (Table 3).

(c) The wetted perimeter (w) was calculated as will be shown in the next section from the values of $\frac{h}{b}$ and A/b^2 .

(d) The slope of the glass bed "S", was measured in degrees and minutes by a clinometer at each section of the channel. It was found that the slope differed from one section to the other, which means that the glass bed was not quite plane.

The second method of measurement was applied to experiments (7 - 15). To obtain results for the earlier experiments (1 - 6) of comparable accuracy, a numerical technique of curve fitting was applied to calculate the area, the depth of flow and the wetted perimeter. This method of interpolation will be explained in section (3.4), and supercedes the graphical method described in section (3.2.1).

3.3 SHAPE OF RUBBER DEFORMED BY WATER PRESSURE

To find the shape of the rubber bed deformed by water pressure, it was treated as a membrane subjected to hydro-static pressure distribution. It was found that the equation of the surface can be described in terms of elliptic functions (see appendix II).

The wetted perimeter is

$$w = \frac{h}{k} K(k) \dots\dots\dots (3.3.1.)$$

where h is the maximum depth, k is a "shape parameter" and K(k) is a complete elliptic integral of first kind.

The width of the free surface is

$$b = \frac{h}{k} [2E(k) - K(k)] \dots\dots\dots (3.3.2.)$$

where E = E(k) is a complete elliptic integral of second kind.

The cross sectional area of the profile is

$$A = \frac{h^2}{k} (1 - k^2) \dots\dots\dots (3.3.3.)$$

and the depth/width ratio is

$$h/b = \frac{k}{(2E - k)} \dots\dots\dots (3.3.4.)$$

Finally θ_0 is the value of θ at the free surface i.e. (the inclination of the tangent plane to the rubber bed at the free surface to the horizontal), then the shape

parameter may be interpreted as

$$k = \sin \frac{\theta_0}{2} \dots\dots\dots (3.3.5.)$$

Values of $(2E)$, (K) , $(2E - K)$ are obtained from the tables of elliptic integrals, and are tabulated in (Table 4), for different values of θ_0 . Table (4) also gives the values of h/b , A/b^2 and w/b . The variation of $\frac{h}{b}$ versus $\frac{A}{b^2}$, and of $\frac{w}{b}$ and $\sec\theta$ versus $\frac{h}{b}$ are all shown graphically in Figure (10).

The experimental values of $\frac{h}{b}$ versus $\frac{A}{b^2}$ are represented on the same figure. It is seen that most of the points lie very close to the theoretical curve. This means that the accuracy of measurement is quite acceptable, and that the theoretical model assumed is adequate.

The values of $\frac{w}{b}$ are obtained from the theoretical curve of $\frac{w}{b}$ versus $\frac{h}{b}$, from which w (the wetted perimeter) is found. The values of h/b , A/b^2 and w/b are tabulated in (Table 5).

It is worthwhile mentioning that A , h and w are the measured values of the cross sectional area, depth and wetted perimeter respectively of the volume of water and rubber sheet together. It is therefore necessary to correct the results to take account of the thickness of the rubber bed.

We make this distinction by giving the measured values of A , h and w , the subscript "m", whilst the corrected values are given subscript "c".

It is then found that

$$h_c = h_m + t(\sec\theta - 1) \quad \text{and} \quad \dots\dots\dots (3.3.6.)$$

$$A_c = A_m + bt \sec\theta - w_m t \quad \dots\dots\dots (3.3.7.)$$

where t is the thickness of the rubber bed which was equal to 0.023", and b is the width of the free surface (see appendix III).

The values of $\frac{w_c}{b}$ are obtained as explained before, but using the values of $\frac{h_c}{b}$ instead of $\frac{h_m}{b}$. The difference between the corrected values and the measured values is very small, as will be seen by comparing the values of $\frac{h_c}{b}$, $\frac{A_c}{b^2}$ and $\sec\theta$ tabulated in (Table 6) with those in (Table 5). These values are represented on the curve of the theoretical variation of $\frac{h}{b}$, $\frac{A}{b^2}$ versus θ (see Figure 10).

3.4

METHOD OF INTERPOLATION

As we have seen in the previous section, the ordinates composing the profile of rubber for experiments (1 - 6), were measured at abscissae different than those of other experiments (7 - 15). The two ordinates at the end points of the free surface were not measured. The point to be made is that the comparison of experimental with the theoretical model showed that the latter was a satisfactory way of deriving values of h/b and w/b from A/b^2 . A numerical formula was then derived to interpolate the values of h/b and A/b^2 . These were found to be consistent once again with the theory (see appendix IV).

The corrected values of h_c/b and A_c/b^2 were calculated as explained before.

4. FREE SURFACE SLOPE, COEFFICIENT OF FRICTION AND

REYNOLDS NUMBER FOR STEADY CHANNEL FLOW

4.1 FREE SURFACE SLOPE

Any point on the free surface could be located with respect to a horizontal datum by adding the distance (z) from the horizontal datum to the rubber bed to the depth of water (h) at the point considered. The height of the free surface point above the horizontal datum is then

$$H = h + z \quad \dots\dots\dots (4.1.1.)$$

Values of h, z and H are tabulated in (Table 7).

The slope of the free surface (i) is theoretically dH/dz , but the data were not sufficiently accurate to allow simple differencing of the measured values of H to obtain this derivative. Instead the least square method was used to fit a straight line to the experimental data for H versus x (see appendix V) and the slope of the regression line was taken as (dH/dz) . This method also permitted assessment of the error of dH/dz so calculated.

It is worthwhile mentioning here that the authors of all references for channel flow treat the velocity over the section as a constant. It follows from that assumption that the energy E_{12} dissipated in unit time in the region between the sections 1 and 2 is equal to

$$\frac{E_{12}}{g\rho} = \iint_1 u(z_1 + h_1 + \frac{u^2}{2g}) dA - \iint_2 u(z_2 + h_2 + \frac{u^2}{2g}) dA$$

$$= Q(z_1 + h_1 - z_2 - h_2) + \iint_1 \frac{u^3}{2g} dA - \iint_2 \frac{u^3}{2g} dA \dots (4.1.2.)$$

Supposing now that the velocity is uniform at each of these sections, i.e. $u = v_1$ at section 1 while $u = v_2$ at section 2. Then (4.1.2.) becomes

$$\frac{E_{12}}{g\rho Q} = z_1 + h_1 - z_2 - h_2 + \frac{v_1^2 - v_2^2}{2g}$$

Let (i) be the gradient of the total head, and let "e" be the energy dissipated in unit length of channel in unit time. Then equation (4.1.2.) is equivalent to

$$e = g\rho Qi \dots \dots \dots (4.1.3.)$$

Now when the velocity is constant across the section e is equal to v multiplied by the resistance of unit length of channel, i.e.

$$e = v \tau m w \dots \dots \dots (4.1.4.)$$

From (4.1.3.) and (4.1.4.)

$$\tau m = g\rho mi \dots \dots \dots (4.1.5.)$$

It is to be understood however, that it is a crude approximation to treat the velocity as constant over the section. This was the reason that the slope of the total head line was treated here by neglecting the change in kinetic energy $\frac{v^2}{2g}$ as described by equation (4.1.1.). The velocity of flow varies at different points of the cross section of the channel. The frictional resistance of the sides causes the water to slow down towards the sides of the channel, and the frictional resistance between the water surface and the atmosphere causes a slight reduction of velocity at the free surface.

Let us consider an element of fluid contained between a pair of normal planes at unit distance apart. (9)
 As the regime is uniform and steady, every fluid particle is unaccelerated and the forces on the element must therefore be in equilibrium. Since the atmospheric pressure at the free surface is assumed to be constant, it follows that the pressures at corresponding points of any two normal sections are the same, so the pressures on the element are themselves in equilibrium. Consequently the component of the weight of the element in the direction of flow must balance the frictional force on the element at the bed of the channel. Let τ be the frictional stress at the bed in the direction of the generators (the direction of mean flow) and let (dw) be an element of the wetted perimeter. Then the total frictional resistance per unit length is

$$\tau dw = w \tau_m, \text{ say } \dots\dots\dots (4.2.1.)$$

where w is the total wetted perimeter and τ_m is the mean frictional stress. The weight of the element is $\rho g A$, where A is the cross sectional area of the channel up to the free surface (the area of the wetted cross section), and the component of the weight in the direction of the flow is $(i \rho g A)$,

Consequently the condition of equilibrium is

$$w \tau_m = i \rho g A$$

$$\tau_m = i \rho g m \dots\dots\dots (4.2.2.)$$

where $m = \frac{A}{w}$ is the hydraulic mean depth

By definition the skin friction coefficient is

$$c_f = \frac{\tau_m}{\frac{1}{2} \rho v^2} \dots\dots\dots (4.2.3.)$$

where v is the mean velocity of flow

It follows that

$$c_f = \frac{2 i g m}{v^2} \dots\dots\dots (4.2.4.)$$

The Reynolds number will be defined here as

$$R = \frac{v m}{\nu} \dots\dots\dots (4.2.5.)$$

where ν is the kinematic viscosity of the fluid

$$R \cdot c_f = \frac{2 i g A^3}{Q \nu w^2} \dots\dots\dots (4.2.6.)$$

We shall next calculate the theoretical values of $(R \cdot c_f)$ for laminar and turbulent flows in an open channel.

4.2.1

LAMINAR FLOW

By the usual assumptions, the equations of motion are taken as (10)

$$\nabla^2 u = - \frac{gi}{\nu} \quad \frac{\partial u}{\partial x} = 0 \quad \dots\dots\dots (4.2.1.1.)$$

where i is the slope of the free surface and u = 0 at the boundaries of the pipe.

The theoretical values of R.cf are derived in (appendix VI) and are found to be

For a parabolic shape, R.cf = $\frac{35}{9}$

For a rectangular shape, R.cf = 6

For a triangular shape, R.cf = 3

4.2.2

TURBULENT FLOW

The Blasius equation for the skin friction of the flow in a smooth pipe of circular cross section is

$$cf = \frac{\tau_m}{\frac{1}{2}\rho v^2} = \frac{0.0791}{\left(\frac{vD}{\nu}\right)^{1/4}} \quad \dots\dots\dots (4.2.2.1.)$$

where D is the diameter of the pipe (equal to 4m).

$$cf = \frac{0.0791}{\left(\frac{4vm}{\nu}\right)^{1/4}} = \frac{0.056}{(R)^{1/4}} \quad \dots\dots\dots (4.2.2.2.)$$

By multiplying cf in equation (4.2.2.2.) by Reynolds number therefore we find the value of

$$R \cdot cf = \left(\frac{R}{48} \right)^{\frac{3}{4}} \dots\dots\dots (4.2.2.3.)$$

which is the theoretical value of R.cf for turbulent flow in open channels.

All the formulae for resistance in perfectly smooth pipes are empirical. The Blasius formula was chosen because of its simplicity.

The experimental values of R versus cf are represented on a graph containing the theoretical values of laminar and turbulent flows in open channels shown in (Fig. 13).

5.

OBSERVATIONS AND RESULTS

5.1

OBSERVATIONS

Three complications affected the experimental results.

- (a) Hydraulic jump.
- (b) Unevenness of the glass bed.
- (c) Unevenness of the rubber bed.

Each of them will be considered separately.

(a)

HYDRAULIC JUMP

It was observed for both groups of experiments (1 - 6) and (7 - 15) that when the water first was allowed to flow down the channel a hydraulic jump was formed approximately half way down the channel. Subsequently within about a minute, the jump seemed to move upstream for a distance of approximately one foot. Only a few small ripples on the free surface of water were observed at distances greater than about a foot downstream from the jump. Measurements of course were not made at positions affected by the jump.

It was also observed that the slope of the channel has a considerable effect on the position of the jump. It was observed for faster flow (with steeper slope), the jump moved downstream, and when the slope was decreased

the jump moved upstream. It is obvious that, if the slope were made smaller or steeper then the jump would vanish completely. Other complications would then arise, because of the supercritical flow in case of steep slopes, and considerable difference in the cross-section of the profile of water from one section to the other in case of very small slopes.

(b) UNEVENESS OF THE GLASS BED

Some measurements were also affected by the unevenness of the glass bed and the two angles supporting the channel, on which the rubber bed was clamped. This unevenness was in both directions, along and across the channel.

An artificial plywood bed having the dimensions 10ft x 12ins x 0.5in, was fixed by G clamps on the glass bed. It helped in minimizing the difference in the slope between one section and another along the channel.

5.3

UNEVENNESS OF THE RUBBER BED

The unevenness of the angles supporting the channel, and on which the rubber bed was clamped affected the evenness of the rubber bed to a certain extent, and accordingly the slope of the rubber bed was also affected. Several attempts were made to make the angles as straight as possible, but there was always some difference between one section and another. Accordingly the measured slope of the free surface (i) was also different from one section to another.

This problem was very difficult to overcome, and the only solution appeared to be a major structural re-design of the channel.

5.4

RESULTS

Values of Reynolds number and the friction coefficient are tabulated in (Table 8). For all the fifteen experiments considered the range of Reynolds number was between 4700 and 935 and the friction coefficient varied from 0.015 to 0.005.

The standard error which is equal to $\sqrt{\frac{\sum s^2_k}{k}}$, was found to be $\pm 274 \times 10^{-6}$, which is about 0.03 of the mean cf.

6.

TESTS WITH THE RUBBER BED BEING TIGHTENED

Other tests were tried where the rubber bed was tightened sufficiently, to ensure that the whole width of the channel was wetted. Two different materials were used for the bed, the first was the same rubber (0.023" thick) used for the previous experiments and the second was another rubber (0.01" thick). With both beds the water flowed in a disturbed state with sinusoidal free surface waves in plan. The bed also oscillated. No measurements were taken because of the unsteadiness of the flow, although it was observed that the wetted perimeter was big and the area of flow was small compared to those in the previous experiments.

If we give a value for the hydraulic mean depth (m) equal to say, 0.02 ft., and a value of v, say, 2 ft/sec., then the value of $\frac{1}{2}\rho v^2 m^2$ will be about 16×10^{-4} lb. Considering first the sheet of rubber 0.023" thick, the corresponding value of $Gt^2/\frac{1}{2}\rho v^2 m^2$ will be about 9.4 and $\frac{t}{m}$ about 0.1, which might place the material in the region where the flexural waves exist. Also with the other material (0.01" thick), the value of $Gt^2/\frac{1}{2}\rho v^2 m^2$ will be about 2 with a value of $\frac{t}{m}$ about 0.04, which might also place the material in the region where the flexural waves exist.

7.

STATISTICAL ANALYSIS AND CONCLUSIONS

7.1

STATISTICAL ANALYSIS

The object of this analysis is to find where the most probable values of Reynolds number for laminar, transition, and turbulent flow are likely to be (see appendix VII). By assuming a normal distribution of observations about the mean, and the values of

$$\overline{cf} - (cf \text{ laminar})_m / S.D., \text{ and } (cf \text{ turbulent})_m - \overline{cf} / S.D.,$$

where

\overline{cf} is the mean experimental value of the friction coefficient, $(cf \text{ laminar})_m$, $(cf \text{ turbulent})_m$, are the calculated values of laminar and smooth turbulent flow friction coefficients at the Reynolds number R_m , and

$$S.D. \text{ is the standard deviation } = \frac{\text{Prob. error}}{0.675},$$

we can calculate $(P \text{ lam})_m$ and $(P \text{ turb})_m$, the probabilities that the experimental results were a sample of measurements in which the skin friction was (respectively) no bigger than that in laminar flow, and no smaller than that in turbulent flow. The probability that the actual skin friction lies between the laminar and turbulent flow values is

$$(P \text{ transition})_m = 1 - (P \text{ laminar})_m - (P \text{ turbulent})_m, \text{ since the sum of the three probabilities is equal to 1.}$$

The values of Reynolds number are arranged in a way such that $R_1 < R_2 < R_3 \dots < R_m$, and the values of the probability for laminar, transition, and turbulent are calculated for $m = 1$, next for $m = 2$, ... etc. For $m = 2$ the probabilities are found to be 6, but this does not represent all the probabilities (that is when added together they do not sum up to unity). There are three probabilities which represent the probability of a decrease in friction as the Reynolds number is increased from R_1 to R_2 . It would seem reasonable to dispose of these as impossible on physical grounds, in which the 6 probabilities defined above must be divided by their total sum (a number less than 1), and these increased values denote the corrected probabilities, ignoring, that is, the possibility of reduction of friction with increased Reynolds number.

The notation is made more convenient by putting
 $(P \text{ lam})_m = P_{1m}$ $(P \text{ trans})_m = P_{2m}$ $(P \text{ turb})_m = P_{3m}$
and calling $P(v, \mu)$ the probability that the friction value is laminar for $R \leq R_v$, and turbulent for $R \geq R_\mu$ where $\mu \geq v + 1$. When the final set of probabilities calculated for $m = N$, say, has been calculated by the above iteration, we have an array of $\frac{1}{2} (N + 1)(N + 2)$ probabilities.

$P(v, \mu)$ where $v = 0, 1 \dots (\mu - 1)$ and $\mu = 1, 2 \dots (N + 1)$,

by tabulating them in a matrix form with each new value of v occupying a row, and each value of μ a column, it should be observable what the most probable values of v and μ are likely to be. Further it should be possible to enclose a range of values of v and μ about the maximum probability value, such that their sum is equal to half. This would then indicate the most probable range of each of the values v and μ , and hence denote the most probable range of R_v , the Reynolds number of transition, and of R_μ the Reynolds number of fully established turbulent flow.

The values of d , $p = \frac{1 - P}{2}$, ⁽¹¹⁾ are tabulated in (Table 9). The values of R_m , cf , $(\partial m . cf)$, $(S.D.)$, $cf(\text{laminar})$, $(cf \text{ turbulent})$, $(d \text{ laminar})$, $(d \text{ turbulent})$, p_{1m} , p_{2m} , and p_{3m} are tabulated in (Table 10).

The final set of probabilities was found by calculations at $m = 7$ which means that the flow is fully turbulent at values of R equal to or more than R_7 see (Table 11). The probabilities are tabulated in a matrix form with each new value of v occupying a row and each value of μ a column (Fig. 11). The probability of the state of flow is represented versus Reynolds number (Fig. 12), by summing the probabilities once in the direction of μ , and once in the direction of v , which gives two curves representing the turbulent and laminar flow respectively,

then by adding the sum of the probabilities in both directions (ν, μ) and subtracting from 1 (since $1 = P \text{ laminar} + P \text{ turbulent} + P \text{ transition}$), we obtain the transition curve. From (Fig. 12), the most probable values of Reynolds number for laminar, transition and turbulent flow can be determined, this is represented in (Fig. 13).

Referring to (Fig. 12), if the 90 per cent probability level is considered, the flow is likely to be laminar at a value of Reynolds number equal to 620, transitional at a value of Reynolds number between 1600 and 1800, and turbulent at a value of Reynolds number equal to 2370. At the 50 per cent probability level, it is observed that the flow can be either laminar or transitional at a value of Reynolds number approximately equal to 1180, and it could be transitional or turbulent at a value of Reynolds number equal to 2280.

Numerous experiments⁽¹²⁾ have shown that the flow in a circular pipe changes from laminar to turbulent at a value of Reynolds number equal to about 2300. In these experiments the diameter of the pipe was taken as the characteristic length in defining the Reynolds number. When the hydraulic mean depth is taken as the characteristic length, the corresponding value is about 500, since the diameter of a pipe is four times its hydraulic mean depth.

The lack of similarity in the shape of the channel considered here, makes it difficult to compare the value of Reynolds number at which transition takes place. It would therefore be necessary to find experimentally the value of Reynolds number for transition

in open channels having say a parabolic rigid bed. This should have been done in the course of the present work, but lack of time did not allow it.

On the whole, it seems doubtful whether the flexible bed maintains the laminar flow, or in other words delays transition, when compared with rigid beds having the same shape.

We can conclude that, if there is any relevance between Nonweiler's criteria for stabilizing the boundary layer in contact with a flexible surface, and the criteria for stabilizing the flow in open channels, the critical value of $\frac{Gt^2}{\frac{1}{2}\rho v^2 m^2}$ must be equal to approximately 250. With soft rubbers of 0.023" thick and a modulus of rigidity of about 33 p.s.i., the value of $\frac{Gt^2}{\frac{1}{2}\rho v^2 m^2}$ will be about 5 and $\frac{t}{m}$ about 0.032. Accordingly the material used may be thought perhaps to be in the region where the flexural waves exist. Therefore, we may suggest using a flexible material which gives exactly the critical value of $\frac{Gt^2}{\frac{1}{2}\rho v^2 m^2}$. The most suitable materials seem to be "Melinex" as explained before in Section 2.1, with a modulus of rigidity of 2×10^5 p.s.i., and a thickness of 0.002". If, on the other hand, aluminium foils with a modulus of rigidity of about 38×10^5 p.s.i., have to be used, then the

thickness must be about 0.0005" in order to satisfy the criteria for the elimination of the Tollmien-Schlichting waves, and the flexural waves, and also the satisfy the criterion for the behaviour like a membrane. If strong rubbers have to be used with a modulus of rigidity of about 4×10^4 p.s.i., then the thickness required will be about 0.005", however, it is difficult to find strong rubbers having this particular thickness. With soft rubbers having a modulus of rigidity of about 33 p.s.i., it seems that the thickness required for satisfying the criterion for the elimination of the Tollmien-Schlichting waves and the flexural waves must be about 0.17", this of course will not satisfy the criteria for the behaviour like a membrane.

8. APPENDICES

APPENDIX I

DEVELOPMENT OF A METHOD FOR MEASURING THE
ORDINATES AT SPECIALLY SELECTED POINTS

Suppose we wish to integrate a function $f(x)$ over the range from $x = -1$ to $+1$, then

$$\int_{-1}^{+1} f(x) dx = \int_0^1 [f(x) + f(-x)] dx \dots\dots (1)$$

$$\text{and } f(x) + f(-x) = 2f(0) + [f(1) - 2f(0) + f(-1)] x^2 + x^2(1 - x^2) g(x^2), \text{ say } \dots\dots\dots (2)$$

since it is an even function of x , let us now write

$$\xi = 2x^2 - 1 \text{ i.e., } x^2 = \frac{1 + \xi}{2} \text{ i.e.,}$$

$$dx = \frac{d\xi}{\frac{3}{2}(1 + \xi)^{\frac{1}{2}}} \dots\dots\dots (3)$$

Then substituting from (3) and (2) in (1),

$$\int_{-1}^{+1} f(x) dx = \frac{4}{3} f(0) + \frac{1}{3} [f(1) + f(-1)] + \int_{-1}^{+1} (1 - \xi)(1 + \xi)^{\frac{1}{2}} h(\xi) d\xi \dots\dots\dots (4)$$

where

$$h(\xi) = 2^{-\frac{7}{2}} g\left(\frac{1+\xi}{2}\right) \dots\dots\dots (5)$$

and from (2)

$$g(t) = \frac{f(t^{\frac{1}{2}}) + f(-t^{\frac{1}{2}}) - 2f(0) - [f(1) + f(-1) - 2f(0)]t}{t(1-t)} \dots\dots\dots (6)$$

If we now suppose that $h(\xi)$ is approximated by a polynomial of degree $(2n - 1)$, which by (2) and (5) is equivalent to considering $g(t)$ to be polynomial of degree $(2n - 1)$, and $f(x)$ to be polynomial of degree $(4n + 3)$, then by the principles of mechanical quadrature (Bateman, Higher Transcendental Functions, Vol. II. McGraw Hill, 1953) in (3).

$$\int_{-1}^{+1} (1 - \xi)(1 + \xi)^{\frac{1}{2}} h(\xi) d\xi = \sum_{\nu=1}^n \lambda_{\nu_n} h(\xi, \nu) \dots\dots (7)$$

where ξ_1, \dots, ξ_n are the zeros of the orthogonal of degree n associated with the weight-function $(1 - \xi)(1 + \xi)^{\frac{1}{2}}$ and λ_{ν_n} are the associated Christoffel numbers. The appropriate orthogonal polynomial is Jacobi's polynomial $P_n(1, \frac{1}{2})(\xi)$.

Pursuing the calculation for $n = 2$ (i.e. approximating $f(x)$ by a polynomial of degree 11), we have

$$\begin{aligned}
P_2^{(1, \frac{1}{2})}(\xi) &= \frac{1}{4} \left[\frac{15}{8}(1 - \xi)^2 - \frac{15}{2}(1 - \xi^2) + 3(1 + \xi)^2 \right] \\
&= \frac{3}{32} [33\xi^2 + 6\xi - 7] \dots\dots\dots (8)
\end{aligned}$$

Thus the zeros are, on equating this expression to zero,

$$\xi_1, \xi_2 = \frac{(-3 \pm \sqrt{240})}{33} \dots\dots\dots (9)$$

$$\xi_1 = 0.3785433$$

$$\xi_2 = -0.5603615$$

The Christoffel numbers λ_{v_n} for the Jacobi Polynomial $P_n^{(\alpha, \beta)}(\xi)$ are given by

$$\begin{aligned}
v_n &= \frac{2^{\alpha + \beta - 1} (n + \alpha - 1)! (n + \beta - 1)! (2n + \alpha + \beta)^2}{n! (n + \alpha + \beta)! (n + \alpha)(n + \beta)} \\
&\times \frac{1 - \xi^2_{v_n}}{[P_{n-1}^{(\alpha, \beta)}(\xi_{v_n})]^2} \dots\dots\dots (10)
\end{aligned}$$

Now

$$\begin{aligned}
P_1^{(1, \frac{1}{2})}(\xi) &= \frac{1}{2} \left[\frac{3}{2}(\xi - 1) + 2(\xi + 1) \right] \\
&= \frac{1}{4}(7\xi + 1) \dots\dots\dots (11)
\end{aligned}$$

and so

$$\lambda_{v_2} = \frac{121}{25} \cdot \frac{2}{21} \frac{11}{2} \frac{(1 - \xi^2 v)}{(1 + 7\xi v)^2} \dots\dots\dots (12)$$

But substituting from equations (5) to (7) and (12) in (4) we have therefore

$$\int_{-1}^{+1} f(x) dx = \left[\frac{4}{3} f(0) + \frac{1}{3} f(1) + f(-1) \right] + \frac{121}{25} \cdot \frac{16}{21} \sum_{v=1}^2 \left\{ f \sqrt{\frac{1 + \xi v}{2}} + f \left(- \sqrt{\frac{1 + \xi v}{2}} \right) - 2f(0) - \left[f(1) + f(-1) - 2f(0) \right] \frac{1 + \xi v}{2} \right\} (1 + 7\xi v)^{-2} \dots\dots\dots (13)$$

where ξ_1 and ξ_2 are given by equation (9). Thus we can write

$$\int_{-1}^{+1} f(x) dx = \sum_{m=1}^7 k_m f(x_m) \dots\dots\dots (14)$$

where

$$x_1 = -1, \quad x_2 = -x_6, \quad x_3 = -x_5, \quad x_4 = 0, \quad x_5 = \left[\frac{15 - \sqrt{60}}{33} \right]^{\frac{1}{2}},$$

$$x_6 = \left[\frac{15 + \sqrt{60}}{33} \right]^{\frac{1}{2}}, \quad x_7 = 1 \dots\dots\dots (15)$$

$$x_3 = -0.468846, \quad x_5 = 0.468846,$$

$$x_2 = -0.830222, \quad x_6 = 0.830222 \quad \text{and where}$$

$$k_1 = k_7 = \frac{1}{3} - \frac{8}{21} \cdot \frac{121}{25} \left[-\frac{1 + \xi_1}{(1 + 7\xi_1)^2} + \frac{1 + \xi_2}{(1 + 7\xi_2)^2} \right]$$

$$= 0.047620$$

$$k_2 = k_6 = \frac{16}{21} \cdot \frac{121}{25} \frac{1}{(1 + 7\xi_1)^2} = 0.2768238$$

$$k_3 = k_5 = \frac{16}{21} \cdot \frac{121}{25} \frac{1}{(1 + 7\xi_2)^2} = 0.431728 \quad (16)$$

$$k_0 = \frac{4}{3} + \frac{121}{25} \cdot \frac{16}{21} \left[\frac{1 + \xi_1}{(1 + 7\xi_1)^2} + \frac{1 + \xi_2}{(1 + 7\xi_2)^2} \right]$$

$$- \frac{32}{21} \cdot \frac{121}{25} \left[\frac{1}{(1 + 7\xi_1)^2} + \frac{1}{(1 + 7\xi_2)^2} \right]$$

$$= 0.487694$$

Substituting from (16) in (14), therefore

$$\int_{-1}^{+1} f(x) dx = k_1(y_1 + y_7) + k_2(y_2 + y_6) + k_3(y_3 + y_5) + k_4 y_4$$

$$= 0.047620(y_1 + y_7) + 0.276823(y_2 + y_6)$$

$$+ 0.431728(y_3 + y_5) + 0.487694(y_4)$$

$$\int_a^c f(x) dx = 0.02381(y_1 + y_7) + 0.13841(y_2 + y_6) \\ + 0.21586(y_3 + y_5) + 0.24384(c - a)$$

$$x_1 = a + 0 = a$$

$$x_2 = a + 0.16978 \left(\frac{c - a}{2} \right) = a + 0.08489$$

$$x_3 = a + 0.53115 \left(\frac{c - a}{2} \right) = a + 0.26557$$

$$x_4 = a + \frac{(c - a)}{2} = a + 0.5(c - a)$$

$$x_5 = a + 1.46885 \left(\frac{c - a}{2} \right) = a + 0.7344(c - a)$$

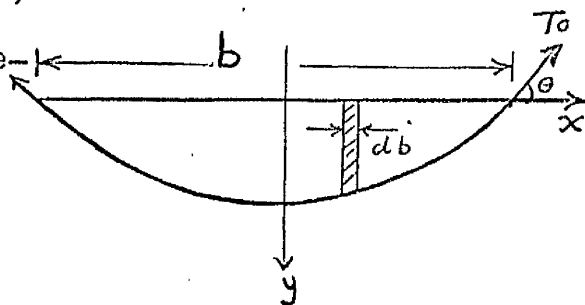
$$x_6 = a + 1.83022 \left(\frac{c - a}{2} \right) = a + 0.91511(c - a)$$

$$x_7 = a + 2 \left(\frac{c - a}{2} \right) = a + (c - a) = c$$

APPENDIX II

SHAPE OF RUBBER DEFORMED BY WATER PRESSURE

Take x - axis in free surface,
 y - axis vertically downwards on centre-
 line. If T_0 is the tension in rubber
 (assumed constant) per unit length and
 $\frac{dy}{dx} = \tan\theta$ (where θ is the inclination
 of rubber to the horizontal) then



$$ds = \sqrt{dx^2 + dy^2} \quad \text{and}$$

$$\frac{d\theta}{ds} = \frac{\Delta P}{T_0} = - \frac{\rho g y}{T_0} = \frac{\frac{d^2y}{dx^2}}{1 + \left[\left(\frac{dy}{dx}\right)^2\right]^{\frac{3}{2}}} \quad \dots\dots\dots (1)$$

where $\frac{d\theta}{ds}$ is the curvature "K" of the elastic curve. This relation bears the name Bernoulli - Euler Law.

Write $P = \frac{dy}{dx}$. $\frac{d^2y}{dx^2} = P \frac{dP}{dy}$.

Substitute in equation (1),

$$- \frac{\rho g y}{T_0} = \frac{P \frac{dP}{dy}}{(1 + P^2)^{\frac{3}{2}}}$$

and by integrating this equation the constant of integration will be

$$C = \frac{1}{(1 + P^2)^{\frac{1}{2}}} - \frac{\rho g y^2}{2T_0} \dots\dots\dots (2)$$

But $y = h, P = 0$

$$\text{therefore } C = 1 - \frac{\rho g h^2}{2T_0} \dots\dots\dots (3)$$

Therefore substitute in (2)

$$\frac{1}{(1 + P^2)^{\frac{1}{2}}} = \frac{\rho g (y^2 - h^2)}{2T_0} + 1 \dots\dots\dots (4)$$

$P = \frac{dy}{dx} = \tan\theta, ds^2 = dy^2 + dx^2$, then ignoring the weight of thickness of rubber itself,

$$\frac{d\theta}{ds} = - \frac{\rho g y}{T_0} \text{ so that if } \eta = \frac{y}{h}, P = \tan\theta \text{ and}$$

$$\frac{\rho g h^2}{4T_0} = k^2 \dots\dots\dots (5)$$

Substitute with the value of $\eta = \frac{y}{h}$ in equation (4)

therefore

$$\frac{1}{(1 + P^2)^{\frac{1}{2}}} = \frac{\rho g (\eta^2 h^2 - h^2)}{2T_0} + 1$$

and by substituting with (5) in (4)

therefore

$$\frac{1}{(1 + P^2)^{\frac{1}{2}}} = 2k^2(\eta^2 - 1) + 1.$$

By differentiation we get

$$- P(1 + P^2)^{-\frac{3}{2}} dP = 4k^2 \eta d\eta$$

By integrating this equation

$$\frac{1}{(1 + P^2)^{\frac{1}{2}}} = 2k^2 \eta^2 + C \dots\dots\dots (6)$$

when $y = h$, $P = 0$, therefore $\eta = 1$

therefore $C = 1 - 2k^2$

Then it follows that

$$(1 + P^2)^{\frac{1}{2}} = 1 - 2k^2(1 - \eta^2)^{-1} \dots\dots (7)$$

$$(1 + P^2)^{\frac{1}{2}} = \sec\theta \quad \text{since } P = \frac{dy}{dx}$$

$$(1 + P^2)^{\frac{1}{2}} = \sec\theta = 1 - 2k^2(1 - \eta^2)^{-1}$$

therefore

$$P = \tan\theta = \pm (1 - \eta^2)^{\frac{1}{2}} \left(\frac{1}{k^2} - 1 + \eta^2 \right)^{\frac{1}{2}} \left(\frac{1}{2k^2} - 1 + \eta^2 \right)^{-1} \dots\dots\dots (8)$$

Now we have $\eta = \frac{y}{h}$,

therefore $d\eta = \frac{dy}{h}$

$$dw = \frac{dy}{\sin\theta} = \frac{d\eta h}{\sin\theta}$$

$$\text{therefore } w = 2h \int_0^1 \frac{d\eta}{\sin\theta}$$

$$P = \tan\theta = \sin\theta \sec\theta$$

therefore

$$w = \frac{h}{k^2} \int_0^1 \frac{d\eta}{(1 - \eta^2)^{\frac{1}{2}} \left(\frac{1}{k^2} - 1 + \eta^2\right)^{\frac{1}{2}}} \dots (9)$$

which is in the form

$$\int_0^x \frac{dx}{\sqrt{a^2 + x^2} \sqrt{b^2 - x^2}} = \frac{1}{\sqrt{a^2 + b^2}} \left\{ K(k) - F(\phi, k) \right\}$$

where

$$\phi = \cos^{-1} \frac{x}{b}, \quad k = \frac{b}{a^2 + b^2}$$

Therefore $w = \frac{h}{k} K(k)$ where $K(k)$ is complete elliptic integral of 1st kind.

$$\text{Also } db = dw \cos\theta = \frac{d\eta}{\sin\theta} h \cos\theta$$

$$\text{therefore } db = d\eta h \cot\theta$$

$$\begin{aligned} \text{therefore } b &= 2h \int_0^1 d\eta \cot\theta \\ &= 2h \int_0^1 \frac{\left(\frac{1}{2k^2} - 1 + \eta^2\right) d\eta}{(1 - \eta^2)^{\frac{1}{2}} \left(\frac{1}{k^2} - 1 + \eta^2\right)^{\frac{1}{2}}} \dots\dots\dots(10) \end{aligned}$$

$$b = 2h \left[\int_0^1 \frac{\left(\frac{1}{2k^2} - 1\right) d\eta}{(1 - \eta^2)^{\frac{1}{2}} \left(\frac{1}{k^2} - 1 + \eta^2\right)^{\frac{1}{2}}} + \int_0^1 \frac{\eta^2 d\eta}{(1 - \eta^2)^{\frac{1}{2}} \left(\frac{1}{k^2} - 1 + \eta^2\right)^{\frac{1}{2}}} \right]$$

$$\begin{aligned}
&= 2h \left\{ \left(\frac{1}{2k^2} - 1 \right) kK(k) + \frac{1}{k} \left[E\left(\frac{\pi}{2}, k\right) - E(0, k) \right] \right. \\
&\quad \left. - \left(\frac{1}{k^2} - 1 \right) k \left[K(k) - F(0, k) \right] \right\} \\
&= 2h \left\{ \left(\frac{1}{2k^2} - 1 \right) kK(k) + \frac{1}{k} E(k) - \left(\frac{1}{k} - k \right) K(k) \right\} \\
&= 2h \left[\frac{2E(k) - K(k)}{2k} \right] \dots\dots\dots (11)
\end{aligned}$$

Therefore $b = \frac{h}{k} \left[2E(k) - K(k) \right]$ where $E(k)$ is complete elliptic integral of 2nd kind.

Also $da = db \cdot y = h^2 \cot\theta \eta d\eta$

$$\begin{aligned}
A &= 2h^2 \int_0^1 \cot\theta \eta d\eta \\
&= 2h^2 \int_0^1 \frac{\eta d\eta}{\left[1 - 2k^2(1 - \eta^2) \right]^{-1} \left[1 - \eta^2 \right]^{\frac{1}{2}} \left[\frac{1}{k^2} - 1 + \eta^2 \right]^{\frac{1}{2}}}
\end{aligned}$$

Put $x = \frac{1}{k^2} (1 - \eta^2)$, $d\eta = -\frac{1}{2}(1 - x)^{-\frac{1}{2}} dx$

$$\text{Therefore } A = h^2 \int_0^1 \frac{\left[\frac{1}{2k^2} - x \right] dx}{\left[x \left(\frac{1}{k^2} - x \right) \right]^{\frac{1}{2}}}$$

$$\text{Therefore } A = \frac{h^2}{k} (1 - k^2)^{\frac{1}{2}} \dots\dots\dots (12)$$

It is evident from considerations of equilibrium that

$$\frac{\rho g A}{2T_0} = \sin \theta_0$$

where θ_0 is the value of θ at the free surface where $\eta = 0$

$$k = \sin \frac{\theta_0}{2} \quad \text{and} \quad \sin \theta_0 = 2 \sin \frac{\theta_0}{2} \cos \frac{\theta_0}{2}$$

Therefore

$$\frac{\rho g A}{4T_0} = \frac{1}{2} \sin \theta_0 = \frac{1}{2} \left[2 \sin \frac{\theta_0}{2} \cos \frac{\theta_0}{2} \right] = k \sqrt{1 - k^2}$$

Therefore
$$A = \frac{4T_0 k \sqrt{1 - k^2}}{\rho g}$$

But from equation (5)
$$\frac{\rho g h^2}{4T_0} = k^2$$

Therefore
$$h^2 = \frac{4T_0 k^2}{\rho g} \quad \text{and} \quad \frac{h^2}{A} = \frac{k}{\sqrt{1 - k^2}} = \tan \frac{\theta_0}{2} \quad (13)$$

Therefore
$$\frac{A}{b^2} = \frac{A}{h^2} \left(\frac{h}{b} \right)^2$$

Therefore
$$\frac{A}{b^2} = \cot \frac{\theta_0}{2} \frac{A \tan \frac{\theta_0}{2}}{\frac{h^2}{k^2} (2E - K)^2}$$

$$= \frac{A k^2}{h^2 (2E - K)^2} = \frac{\cos \frac{\theta_0}{2} \sin \frac{\theta_0}{2}}{(2E - K)^2}$$

Therefore

$$\frac{A}{b^2} = \frac{\sin\theta_0}{2 [2E - K]^2} = \frac{k \sqrt{1 - k^2}}{(2E - K)^2} = \left(\frac{h}{b}\right)^2 \sqrt{\frac{1 - k^2}{k}}$$

Therefore

$$\left(\frac{h}{b}\right)^2 = \frac{A}{b^2} \frac{k}{\sqrt{1 - k^2}} = \frac{k \sqrt{1 - k^2}}{(2E - K)^2} \frac{k}{\sqrt{1 - k^2}} = \frac{k^2}{(2E - K)^2}$$

Therefore

$$\frac{h}{b} = \frac{k}{(2E - K)} = \frac{\sin\frac{\theta_0}{2}}{(2E - K)} \dots\dots\dots (14)$$

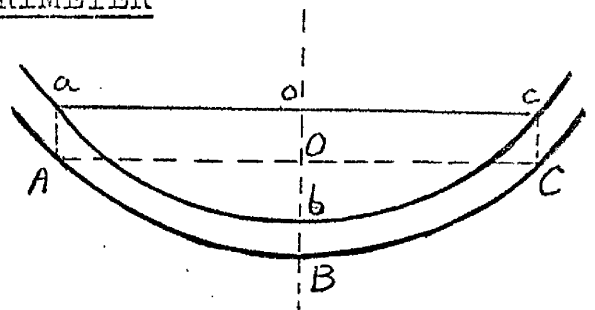
From equation (9), (10) it follows that

$$\frac{w}{b} = \frac{h K(k) k}{kh [2E(k - K(k))]}$$

Therefore $\frac{w}{b} = \frac{K}{[2E - k]} \dots\dots\dots (15)$

APPENDIX III

CORRECTION FOR THE AREA, DEPTH OF FLOW
AND THE WETTED PERIMETER



Let $y = f(x)$ denote vertical ordinates of lower surface of rubber ABC, below the free surface of water aoc. The

experiments measure ordinates

below AOC, where $Aa = Oo = Cc = t \sec\theta_0$ and t is the thickness of rubber.

θ_0 is the slope of the rubber to the horizontal at A and C. Thus if y_m are the measured ordinates, therefore

$$y_m = f(x) - t \sec\theta_0 \quad \dots\dots\dots (1)$$

If y_c are the ordinates of the upper surface of the rubber (i.e. the bottom of the water abc) below the free surface, then

$$y_c = f(x) - t \sec\theta \quad \dots\dots\dots (2)$$

where θ is the local slope of the surface to the horizontal. Thus the measured depth, from (1) and (2) is given by h_m where

$$h_m = f \frac{(a + c)}{2} - t \sec\theta_0 = h_c + t(1 - \sec\theta_0)$$

and h_c is the corrected depth, i.e.

$$h_c = h_m + t(\sec\theta_o - 1) \dots\dots\dots (3)$$

The measured area A_m is that of AOCBA which is given by

$$A_m = \int_a^c y_m dx = \int_a^c f(x) dx - bt \sec\theta_o$$

whereas the correct area is

$$A_c = \int_a^c y_c dx = \int_a^c f(x) dx - t \int_a^c \sec\theta dx$$

Thus, since $\int_a^c \sec\theta dx$ is to the first approximation w , the measured or corrected perimeter is

$$A_c = A_m + bt \sec\theta_o - wt \dots\dots\dots (4)$$

The corrections (3), (4) were found to be very small and to obtain them we needed values of w , θ_o , which were found by fitting the experimentally measured values of $\frac{h_m}{b}$ or $\frac{A_m}{b^2}$ with the theoretical curve. The

corrected values of $w = w_c$ were found by using the corrected values of $\frac{h_c}{b}$ or $\frac{A_c}{b^2}$, thus if according to

theory

$$\frac{w}{b} = g \frac{h}{b} \quad \text{then} \quad \frac{w_c}{b} = g \frac{h_c}{b} \dots\dots\dots (5)$$

but it is adequate in equation (3), (4) to treat

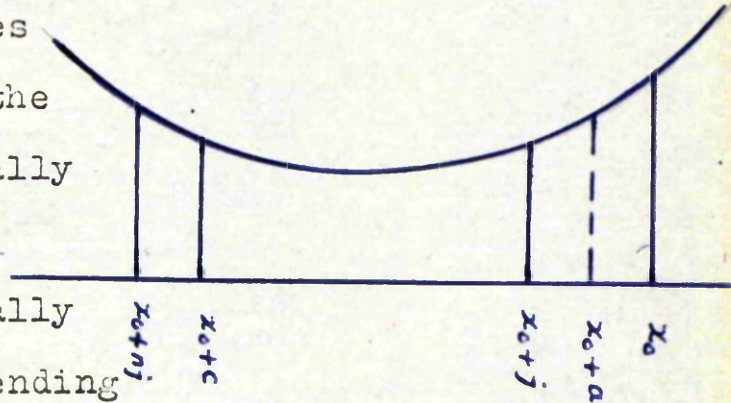
$$\theta_0 = F \frac{h_m}{b} \quad \text{if } \theta_0 = F \frac{h}{b} \quad \text{according to theory} \quad \dots\dots\dots (6)$$

It has been proposed that values of $\frac{h}{b}$ as in (5), (6) be used in preference to $\frac{A}{b^2}$.

APPENDIX IV

METHOD OF INTERPOLATION

We know the ordinates $y_0, y_1, y_2 \dots y_n$ above the datum line at a number of equally spaced abscissae $x_0, x_0 + j, x_0 + 2j, \dots x_0 + nj$. Generally $j = 1$ inch and $n = 4$ or 6 depending on the amount of flow.



Further we know the abscissae of the end points of the free surface $(x_0 + a), (x_0 + c)$, where $c > a > 0$ and $(c - a) = b$. Generally $a < j$ and $nj > c > (n - 1)j$. Let us write

$$\theta = \frac{x - x_0}{nj} \pi$$

and then $\theta_\mu = \frac{\mu\pi}{n}$ corresponds to $x = x_0 + \mu j$, and let us suppose that we interpolate for the variation of the ordinates by the expression

$$Y(x) \equiv Y = y_0 + (y_n - y_0) \frac{\theta}{\pi} + \frac{2}{n} \sum_{\mu=1}^{n-1} B_\mu \sum_{\lambda=1}^{n-1} \sin \lambda \theta_\mu \sin \lambda \theta + 2bc \sin n\theta \dots \dots \dots (1)$$

where the coefficients B_1, B_2, \dots, B_{n-1} and c have yet to be determined.

Using the identity

$$2 \sum_{\lambda=0}^m \cos \lambda \phi = 1 + \cos m\phi + \cot \frac{\phi}{2} \sin m\phi$$

it follows that

$$\begin{aligned} 2 \sum_{\lambda=1}^{n-1} \sin \lambda \theta_{\mu} \sin \lambda \theta &= \sum_{\lambda=0}^n \left[\cos \lambda(\theta - \theta_{\mu}) - \cos \lambda(\theta + \theta_{\mu}) \right] \\ &= \frac{1}{2}(-1)^{\mu} \sin n\theta \left[\cot \frac{1}{2}(\theta - \frac{\mu\pi}{n}) - \cot \frac{1}{2}(\theta + \frac{\mu\pi}{n}) \right] \\ &= \frac{(-1)^{\mu} \sin n\theta \sin \frac{\mu\pi}{n}}{(\cos \frac{\mu\pi}{n} - \cos \theta)} \dots \dots \dots (2) \end{aligned}$$

Thus since $y \rightarrow y_{\mu}$ as $\theta \rightarrow \frac{\mu\pi}{n}$, we see that in (1), using (2) and letting $\theta \rightarrow \frac{\mu\pi}{n}$

$$y_{\mu} - y_0 - (y_n - y_0) \frac{\mu}{n} = B_{\mu} \dots \dots \dots (3)$$

for $\mu = 1, 2, \dots, (n-1)$. Accordingly, only c is indeterminate. The uncorrected depth is given by

$$h = \frac{Y}{2}(x_0 + a) + \frac{Y}{2}(x_0 + c) - Y(x_0 + \frac{c}{2} + \frac{a}{2}) \dots \dots (4)$$

where $Y(x)$ is the interpolated value of y corresponding to abscissa x .

Thus using (1) and (4)

$$\frac{h}{b} = \frac{1}{nb} \sum_{\lambda=1}^{n-1} \sum_{\mu=1}^{n-1} B_{\mu} \sin \lambda \theta_{\mu} \left[\sin \frac{\lambda a \pi}{nj} + \sin \frac{\lambda c \pi}{nj} - 2 \sin \frac{\lambda(a+c)\pi}{2nj} \right] + C \left[\sin \frac{a\pi}{j} + \sin \frac{c\pi}{j} - 2 \sin \frac{(a+c)\pi}{2j} \right] \dots \dots \dots (5)$$

Also the uncorrected area is given by

$$A = \int_{x_0+a}^{x_0+c} \left\{ Y(x_0 + a) + \frac{x - x_0 - a}{b} \left[Y(x_0 + c) - Y(x_0 + a) \right] - y \right\} dx \dots \dots \dots (6)$$

and substituting from (1) it follows that

$$\frac{A}{b^2} = \frac{1}{nb} \sum_{\lambda=1}^{n-1} \sum_{\mu=1}^{n-1} B_{\mu} \sin \lambda \theta_{\mu} \left[\sin \frac{\lambda a \pi}{nj} + \sin \frac{\lambda c \pi}{nj} - 2 \frac{2nj}{\pi b} \sin \frac{\lambda b \pi}{2nj} \sin \frac{\lambda(a+c)\pi}{2nj} \right] + C \left[\sin \frac{a\pi}{j} + \sin \frac{c\pi}{j} - 2 \frac{2j}{\pi b} \sin \frac{b\pi}{2j} \sin \frac{(a+c)\pi}{2j} \right] \dots \dots \dots (7)$$

Both $\frac{h}{b}$ and $\frac{A}{b^2}$ are accordingly linearly

dependent on C, and consequently, plotting $\frac{h}{b}$ versus $\frac{A}{b^2}$, we find that the curve representing the possible interpolated values is a straight line, the appropriate values being given by the intersection of this straight line with the theoretical curve.

For computation, the square array of values of $\sin \lambda \theta_{\mu} = \sin(\lambda \mu) \left(\frac{\pi}{n}\right)$ was worked out for $n = 4$ and $n = 6$ and was arranged as follows:-

For n = 6

$\lambda \backslash \mu =$	1	2	3	4	5
1	0.5	0.866	1	0.866	0.5
2	0.866	0.866	0	-0.866	-0.866
3	1	0	-1	0	1
4	0.866	-0.866	0	0.866	-0.866
5	0.5	-0.866	1	-0.866	0.5

For n = 4

$\lambda \backslash \mu =$	1	2	3
1	0.707	1	0.707
2	1	0	-1
3	0.707	-1	0.707

(It is noted that the array is symmetrical, the element $S_{\lambda \mu} = \sin \lambda \theta_{\mu}$ being equal to the element $S_{\mu \lambda} = \sin \mu \theta_{\lambda}$.)

Then for a fixed profile, from (3) the values of $\frac{B}{nb} \mu$ for $\mu = 1, 2, \dots (n - 1)$, and

$$h_{\lambda} = \sin \frac{\lambda a \pi}{n j} + \sin \frac{\lambda c \pi}{n j} - 2 \sin \frac{\lambda(a+c)\pi}{2n j}$$

$$A_{\lambda} = \sin \frac{\lambda a \pi}{n j} + \sin \frac{\lambda c \pi}{n j} - 2 \sin \frac{\lambda(a+c)\pi}{2n j} \frac{2n j}{\pi \lambda b} \sin \frac{\lambda b \pi}{2n j}$$

are calculated for $\lambda = 1, 2, \dots, n$.

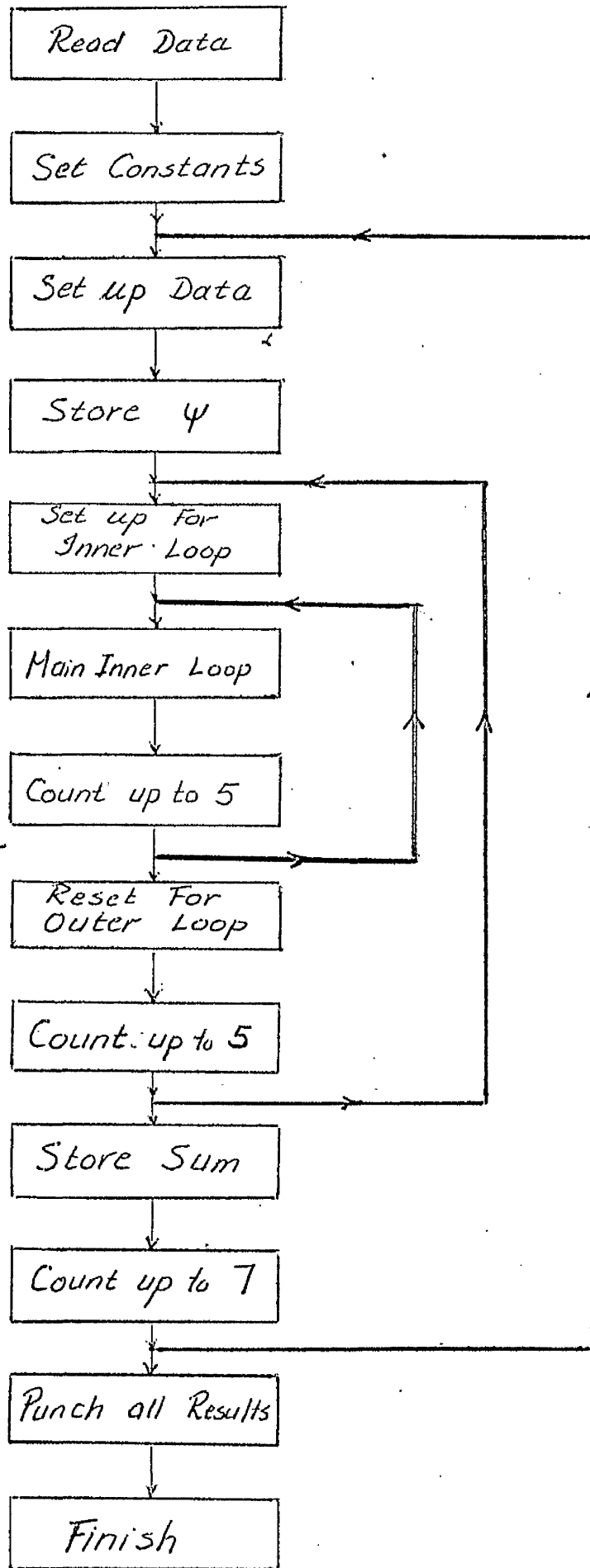
The values of $\frac{h}{b}$ and $\frac{A}{b^2}$ are then from (5) and (7)

$$\begin{aligned} \frac{h}{b} &= \sum_{\lambda=1}^{n-1} \sum_{\mu=1}^{n-1} \frac{B_{\mu}}{n b} h_{\lambda} S_{\lambda \mu} + c h n \dots \dots \dots (8) \\ \frac{A}{b^2} &= \sum_{\lambda=1}^{n-1} \sum_{\mu=1}^{n-1} \frac{B_{\mu}}{n b} A_{\lambda} S_{\lambda \mu} + c A n \end{aligned}$$

and the summations were carried out by multiplying each element of the array $S_{\lambda \mu}$ by the value of $\frac{B_{\mu}}{n b}$ and h_{λ} (or A_{λ}) appropriate to its row and column respectively and adding cumulatively. Placing (say) $c = 0$ immediately gives one possible pair, and (say) $c = 1$ gives another pair of values of h and A , plotting these two values on a graph of $\frac{h}{b}$ and $\frac{A}{b^2}$, and joining by a straight line, enables the intersection to be found. Therefore the values of $\frac{h_m}{b}$ and $\frac{A_m}{b^2}$ were known.

Attached to this appendix is a computer programme using the Deuce Alphacode which was used for calculating these operations.

FLOW DIAGRAM



Notes :

Data : y_0, y_n, y_{2n}

($n = 1, 2, 3, 4, \dots, 6$)

and a, b, c

Constants :

Numerical Figures

$$\psi = \sin \frac{a\pi}{j} + \sin \frac{c\pi}{j} - 2 \sin \left(\frac{a+c}{2} \pi \right)$$

Inner Loop

For v from 1 to 5

Outer Loop

For λ from 1 to 5

APPENDIX V

FREE SURFACE SLOPE AND PROBABLE ERRORS

A straight line equation (an + b) was fitted to (h + z). The sum of the squares of the vertical deviations of the plotted points from this line was made as small as possible

i.e. $\sum_{n=1}^k (h + z - an - b)^2$ was made a minimum with respect to a and b

i.e.
$$\frac{\partial \sum (h + z - an - b)^2}{\partial a} = 0$$

and
$$\frac{\partial \sum (h + z - an - b)^2}{\partial b} = 0$$

then
$$a \sum_{n=1}^K n^2 + b \sum_{n=1}^K n = \sum_{n=1}^K n(h + z) \dots\dots\dots (1)$$

and
$$a \sum_{n=1}^K n + bk = \sum_{n=1}^K (h + z) \dots\dots\dots (2)$$

From (1), (2) it follows that

$$a = \frac{k \sum_{n=1}^K [n(h + z)] - \left(\sum_{n=1}^K n\right) \left[\sum_{n=1}^K (h + z)\right]}{\left(\sum_{n=1}^K n^2\right) k - \left(\sum_{n=1}^K n\right)^2} \dots\dots\dots (3)$$

But $\sum_{n=1}^k n = \frac{1}{2} k(k + 1)$

and $\sum_{n=1}^k n^2 = \frac{1}{6} k(1 + k)(1 + 2k)$

and so substituting with equations (4), (5) in equation (3) we therefore find

$$a = \frac{\frac{1}{k} \left\{ \sum_{n=1}^k n(h + z) - \frac{1}{2}(k + 1) \sum_{n=1}^k (h + z) \right\}}{\frac{1}{12}(k^2 - 1)}$$

$$= - \frac{6}{k(k^2 - 1)} \left\{ (k + 1) \sum_{n=1}^k (h + z) - 2 \sum_{n=1}^k n(h + z) \right\}$$

$$= - \frac{6}{k(k^2 - 1)} \sum_{n=1}^k (k + 1 - 2n)(h + z + c)$$

i.e. $a = \frac{d(h + z)}{dx}$ if (h + z) is in feet.

Therefore $i = a = \frac{6}{k(k^2 - 1)} \sum_{n=1}^k (2n - k - 1)(h + z + c)$

where c is arbitrary.

Also we require the value of b which is obtained by substituting in either of equations (1) or (2) with the value of a

Therefore

$$b = \frac{\sum_{n=1}^k n^2 \left[\sum_{n=1}^k (h + z) \right] - \left(\sum_{n=1}^k n \right) \left[\sum_{n=1}^k n(h + z) \right]}{\frac{k^2(k^2 - 1)}{12}}$$

$$= \frac{2}{k(k - 1)} \sum_{n=1}^k (2k + 1 - 3n)(h + z + c)$$

a and b are used in the expression for the variance

$$V_{H/x} = \frac{1}{k - 2} \sum_{n=1}^k (H_n - a_k n - b_k)^2$$

which is the "variance" of the observations H_n about the "regression line" given by $H = a_k n + b_k$, of H on n .

Interest in this data is restricted to the value of a_k and its significance in determining the true value of

$$i = \frac{\partial H}{\partial x}$$

$$S_a = \left[\frac{12V_{H/x}}{k(k^2 - 1)} \right]^{\frac{1}{2}} \quad \text{is the "standard$$

deviation" of the value a_k .

f	2	3	4	5	6	7	8	9
$t_{\frac{1}{2}}(f)$	1.000	0.816	0.764	0.741	0.727	0.718	0.712	0.707

The value of $t_{\frac{1}{2}}(k - 1)S_a$ is the probable error of the coefficient a_k .

$$\text{Probable error in } Rc_f = \frac{Rc_f t_{\frac{1}{2}} S_a}{i}$$

- 11 -

APPENDIX VI

COEFFICIENT OF FRICTION FOR STEADY CHANNEL FLOW

From the Navier-Stokes equations of motion we know that

$$\frac{\partial u}{\partial t} + u \frac{\partial u}{\partial x} + v \frac{\partial u}{\partial y} + w \frac{\partial u}{\partial z} = - \frac{1}{\rho} \frac{\partial p}{\partial x} + X + \nu \nabla^2 u \quad \dots\dots (1)$$

X is the component of the external force F acting on the fluid per unit of mass.

ρ is the density of the fluid.

Now we consider a steady motion between two fixed parallel planes under the action of a constant pressure gradient, the position of the plane is $y = \pm h$, and the flow is in the direction of the x axis.

Assume that the velocities are

$$u = u(y), \quad v = 0, \quad w = 0$$

From equation (1) we find

$$- \frac{1}{\rho} \frac{dp}{dx} + \nu \nabla^2 u = 0 \quad \text{since } \nu = \frac{\mu}{\rho}$$

$$\text{i.e.} \quad \frac{1}{\mu} \frac{dp}{dx} = \frac{d^2 u}{dy^2} \quad \dots\dots\dots (2)$$

$$\text{therefore} \quad \nabla^2 u = - \frac{gi}{\nu}, \quad \frac{\partial u}{\partial x} = 0$$

where i is the slope of the free surface = $-\frac{1}{\rho g} \frac{dp}{dx}$

The boundary conditions on the planes are (no slip)

$$u = 0 \quad \text{at} \quad y = \pm h$$

whence integrating (2) we find

$$\begin{aligned} u &= -\frac{1}{2\mu} \frac{dp}{dx} (h^2 - y^2) \\ &= \frac{ig(h^2 - y^2)}{2\nu} \dots\dots\dots (3) \end{aligned}$$

we have $w \tau_m = \rho g i A$ or $\tau_m = \rho g m i$

where $m = \frac{A}{w}$ = hydraulic mean depth.

Therefore if

$$R = \frac{Q}{vw} = \frac{vm}{\nu}$$

$$\frac{R \tau_m}{\frac{1}{2}\rho v^2} = \frac{Q}{vw} \frac{\rho g A i}{w} \frac{2A^2}{\rho Q^2} = \frac{2igA^3}{\nu Q w^2} = R_{c_f} \dots\dots\dots (4)$$

Now $dQ = u \, dA = u \, dy \, dz$ therefore

$$Q = \int_0^w \int_0^h u \, dy \, dz$$

$$= \int_0^w \int_0^h \frac{gi(h^2 - y^2)}{2\nu} \, dy \, dz$$

$$= \frac{gi}{2\nu} \int_0^w (h^3 - \frac{h^3}{3}) \, dz$$

$$Q = \frac{g_i}{3\nu} \int_0^w h^3 dz \dots\dots\dots (5)$$

by substituting the values of A, Q in equation (4) we get

$$Rc_f = \frac{6 \left[\int_0^w h dz \right]^3}{w^2 \int_0^w h^3 dz} \dots\dots\dots (6)$$

Now for a rectangular section h is constant, and therefore from (6)

$$Rc_f = 6$$

for a triangular section

$$h = \frac{1}{2} \left[1 - \frac{z}{w} \right] \text{ and therefore from (6)}$$

$$Rc_f = 3$$

and for a parabolic section $h = 0$ at $z = 0$ and $z = w$

$$\text{therefore } h \propto \frac{w^2}{4} - \left(z - \frac{w}{2} \right)^2 = z(w - z) \text{ and from (6)}$$

$$Rc_f = \frac{35}{9} \text{ which is very close to the}$$

value $Rc_f = 4$ for a semi-circular section.

APPENDIX VIISTATISTICAL ANALYSIS

Let \bar{c}_f be the mean value of the friction coefficient based on the experimental results at Reynolds number R_m ($m = 1, 2, 3, \dots, R_1 < R_2 < R_3$) and let δ_m be the corresponding probable error. Further let $(c_f \text{ laminar})_m$ and $(c_f \text{ turbulent})_m$ be the calculated values of laminar and smooth turbulent flow friction coefficients at the Reynolds number R_m . Then the values of $\left[\bar{c}_f - (c_f \text{ laminar})_m \right] / \text{S.D.}$ and $\left[(c_f \text{ turbulent})_m - \bar{c}_f \right] / \text{S.D.}$ (where S.D. is the standard deviation $= \frac{\text{Probable error}}{0.675}$), allow us, by assuming a normal distribution of observations about the mean, to calculate respectively $(p_{\text{lam.}})_m$ and $(p_{\text{turb.}})_m$, the probabilities that the experimental results were a sample of a measurement in which the skin friction was (respectively) no bigger than that in laminar flow, and no smaller than that in turbulent flow. The value of $(p_{\text{transition}})_m = 1 - (p_{\text{lam.}})_m - (p_{\text{turb.}})_m$ then is the probability that the actual skin friction lies between the laminar and turbulent flow values.

The values of $(p_{\text{lam.}})_m$, $(p_{\text{trans.}})_m$ and $(p_{\text{turb.}})_m$ were calculated for $m = 1$, next for $m = 2$,

then the probability that the skin friction was less than or equal to the laminar flow value over the range of Reynolds number from R_1 to R_2 is $(p_{lam.})_1 \times (p_{lam.})_2$

that it was laminar at R_1 , but in the transition range at R_2 , is $(p_{lam.})_1 \times (p_{trans.})_2$

that it was laminar at R_1 , but not less than the turbulent value at R_2 is

$$(p_{lam.})_1 \times (p_{turb.})_2$$

that it was in the transition range for both R_1 and R_2 is

$$(p_{trans.})_1 \times (p_{trans.})_2$$

that it was in the transition range for R_1 but turbulent at R_2 is

$$(p_{trans.})_1 \times (p_{turb.})_2$$

that it was in the turbulent at both R_1 and R_2 is

$$(p_{turb.})_1 \times (p_{turb.})_2$$

These six probabilities do not represent all the possibilities (that is, when added together they do not sum up to unity). There are the three possibilities represent by the products

$$(p_{turb.})_1 \times (p_{trans.})_2, (p_{turb.})_1 \times (p_{lam.})_2,$$

$$(p_{trans.})_1 \times (p_{lam.})_2$$

which represent the probability of a decrease in friction as the Reynolds number is increased from R_1 to R_2 , it would seem reasonable to dispose of these as impossible

on physical grounds, in which event the six probabilities defined above must be divided by their total sum (a number less than 1) and these increased values denote the corrected probabilities, ignoring that is the possibility of reduction of friction with increased Reynolds number. The notation is made more convenient by putting $(p_{\text{lam.}})_m = p_{1m}$, $(p_{\text{trans.}})_m = p_{2m}$, $(p_{\text{turb.}})_m = p_{3m}$ and calling $P(\nu, \mu)$ the probability that the friction value is laminar for $R \leq R_\nu$, and turbulent for $R \geq R_\mu$, where $\mu \geq \nu + 1$.

Then the above results can be summarised as

$$\begin{aligned}
 P(2, \mu_3) &= p_{11} p_{12} / \sum_{j=1}^3 \sum_{k=j}^3 p_{j1} p_{k2} \\
 P(1, \mu_3) &= p_{11} p_{22} / \text{ " " " " } \\
 P(0, \mu_3) &= p_{21} p_{32} / \text{ " " " " } \\
 P(1, 2) &= p_{11} p_{32} / \text{ " " " " } \\
 P(0, 2) &= p_{21} p_{32} / \text{ " " " " } \\
 P(0, 1) &= p_{31} p_{32} / \text{ " " " " }
 \end{aligned}$$

where R_0 denotes some (unknown) value of $R < R_1$.

Next the results for m_3 were considered, and the calculated probabilities p_{13} , p_{23} , p_{33} , the acceptable probabilities were, when uncorrected (denoted by a dash) :-

$$\begin{aligned}
P'(3, \mu_4) &= p_{13} P(2, 3) \\
P'(2, \mu_4) &= p_{23} P(2, 3) \\
P'(1, \mu_4) &= p_{23} P(1, 3) \\
P'(0, \mu_4) &= p_{23} P(0, 3) \\
P'(2, 3) &= p_{33} P(2, 3) \\
P'(1, 3) &= p_{33} P(1, 3) \\
P'(0, 3) &= p_{33} P(0, 3) \\
P'(1, 2) &= p_{33} P(1, 2) \\
P'(0, 2) &= p_{33} P(0, 2) \\
P'(0, 1) &= p_{33} P(0, 1)
\end{aligned}$$

The values of P' were summed and each value of P was divided by this number to find the corrected value $P(3, \mu_4)$, $P(2, \mu_4)$, etc. In general for any value of m

$$\begin{aligned}
P'(m, m + 1) &= p_{1m} P(m - 1, m) \\
P'(m - k, m + 1) &= p_{2m} P(m - k, m) \text{ for } k = 1, 2, \dots, m \\
P'(m - k, m - j) &= p_{3m} P(m - k, m - j)
\end{aligned}$$

for $j = 0, 1, \dots, (k - 1)$ and $k = 1, 2, \dots, m$ where it is understood that $P'(m, m + 1)$ or $P(m - k, m)$ are identical to what in the previous notation would be called $P'(m, m + \mu_m)$ or $P(m - k, m - 1 + \mu_m - 1)$. In this way we use p_{1m} to calculate one new uncorrected probability $P'(m, m + 1)$, we use p_{2m} to calculate m new uncorrected probabilities, and p_{3m} to calculate $\frac{m}{2}(m + 1)$

new uncorrected probabilities, making $\frac{1}{2}(m + 1)(m + 2)$ in all. All these uncorrected probabilities are added together to find their sum $\sum m$, say, and then $P(m, m + 1) = \frac{P'(m, m + 1)}{\sum m}$, etc., and then m increased by one to find a new set.

When the final set of probabilities calculated for $m = N$, say, has been determined by the above iteration, we have an array of $\frac{1}{2}(N + 1)(N + 2)$ probabilities.

$P(v, \mu)$ where $v = 0, 1, \dots (\mu - 1)$ and $\mu = 1, 2, \dots (N + 1)$. By tabulating them in a matrix form with each new value of v occupying a row, and each value of μ a column (see Fig. 11), it should be observable what the most probable values of v and μ are likely to be. Further it should be possible to enclose a range of values of v and μ about the maximum probability value, such that their sum is equal to half. This would then indicate the most probable range of each of the values v and μ , and hence denote the most probable range of R_v , the Reynolds number of transition, and of R_μ the Reynolds number of fully established turbulent flow.

REFERENCES

1. M.O. Kramer. Boundary layer stabilization by distributed damping. Readers forum, J. Aero. Sci. 24, 459, June 1957.
2. M.O. Kramer. Boundary layer stabilization by distributed damping. J. Aero. Sci. 27, 69, January 1960.
3. M.O. Kramer. Boundary layer stabilization by distributed damping. Readers forum, J. Am. Soci. Naval Engrs. 72, 25, February 1960.
4. M.O. Kramer. The Dolphin's Secret. The New Scientist, 1118, 5th May 1960.
5. T.R.F. Nonweiler. Qualitative solution of the stability equation for a boundary layer in contact with various forms of flexible surface. Aeronautical Research Council C.P. No. 622, 1963.
6. H.M. James,
E. Guth. Theory of the elastic properties of rubber. J. Chem. Phy. 11, 455, 1943.
7. Turner Alfrey, J.R. Mechanical behaviour of high polymers. Interscience Publishers, Inc.
8. Jahnke-Emde. Tables of functions, p.78, 80, 1938. Published by B.G. Teubner - Leipzig and Berlin, 1938.

9. W.J. Duncan, A.S. Thom, The mechanics of fluids,
P. 407, 425, 430, 431.
A.D. Young.
10. D. Meksyn. New methods in laminar
Boundary layer theory,
p, 18, 1961.
11. Quenouille. Rapid statistical
calculations, Table (1).
12. Chow. Open channel hydraulics.
P. 8, 1959. McGraw - Hill.

LOAD l_0	L = extended length inches	$\Delta L = L - l_0$ inches	$\frac{\Delta L}{l_0}$ = strain	stress = $\frac{P}{A}$ (area) P.S.I.	E = Young's Modulus P.S.I.	% elongation $\frac{\Delta L}{l_0} \times 100$
0.100	20.840	0.840	0.042	4.35	103.57	4.2
0.200	21.700	1.700	0.085	8.70	102.35	8.5
0.300	22.560	2.560	0.128	13.05	101.95	12.8
0.400	23.480	3.480	0.174	17.40	100.00	17.4
0.500	24.480	4.480	0.224	21.78	97.23	22.4
0.600	25.640	5.640	0.282	26.10	92.55	28.2
0.700	27.100	7.100	0.355	30.40	85.63	35.5
0.800	28.800	8.800	0.440	34.80	79.09	44.0
0.900	30.760	10.760	0.538	39.20	72.86	53.8
1.000	34.500	14.500	0.725	43.50	60.00	72.5

TABLE 1.

THE ORIGINAL LENGTH = 20"

THE CROSS SECTIONAL AREA IS CONSTANT
AND EQUAL TO 0.023 SQUARE INCH.

TABLE 2

EXP. No.	SEC.	$\bar{y} = (y_1 + y_7)/2$	$\bar{y} - y_1 = f(x_1)$	$\bar{y} - y_2 = f(x_2)$	$\bar{y} - y_3 = f(x_3)$	$\bar{y} - y_4 = f(x_4)$	$\bar{y} - y_5 = f(x_5)$	$\bar{y} - y_6 = f(x_6)$	$\bar{y} - y_7 = f(x_7)$
7	2'	1.7505	-0.0065	0.3985	0.9495	1.2265	0.9455	0.3165	0.0065
	3'	1.6425	-0.0255	0.4035	1.0035	1.3105	1.0305	0.4025	0.0255
	4'	1.5905	-0.0205	0.4175	1.0305	1.3505	1.0625	0.4345	0.0205
	5'	1.5495	-0.0165	0.4535	1.0835	1.4135	1.1535	0.5275	0.0165
	6'	1.4720	0.0090	0.4720	1.0920	1.3910	1.0800	0.4140	0.0090
	7'	1.4185	0.0045	0.4665	1.0885	1.4055	1.1335	0.5015	0.0045
	8'	1.3885	-0.0105	0.4205	1.0235	1.3145	1.0235	0.4025	0.0105
	9'	1.2945	-0.0095	0.3805	0.9145	1.1945	0.9295	0.3565	0.0095
	10'	1.2450	-0.0080	0.4000	0.9530	1.2230	0.9450	0.3500	0.0080
	8	2'	1.7045	-0.0105	0.3795	0.9005	1.1755	0.9145	0.3545
3'		1.5705	-0.0305	0.3795	0.9325	1.2185	0.9605	0.3815	0.0305
4'		1.5195	-0.0205	0.4015	0.9745	1.2605	0.9905	0.3795	0.0205
5'		1.4550	-0.0180	0.4100	0.9990	1.3000	1.0220	0.3880	0.0180
6'		1.3570	-0.0100	0.3960	0.9620	1.2460	0.9760	0.3720	0.0100
7'		1.2820	0.0030	0.4120	0.9590	1.2290	0.9510	0.5660	-0.0030
8'		1.1550	-0.0290	0.3010	0.8000	1.0680	0.8460	0.3390	0.0290
9		2'	1.6960	-0.0310	0.1660	0.8560	1.1380	0.8960	0.3590
	3'	1.6310	-0.0210	0.4070	0.9720	1.2600	0.9860	0.3880	0.0210
	4'	1.5520	-0.0430	0.3860	0.9620	1.2720	1.0100	0.4160	0.0430
	5'	1.5100	-0.0200	0.4230	1.0300	1.3310	1.0490	0.4090	0.0200
	6'	1.4505	-0.0195	0.4195	1.0305	1.3305	1.0405	0.4075	0.0195
	7'	1.3975	-0.0175	0.4325	1.0415	1.3415	1.0525	0.4125	0.0175

TABLE 2 Continued.

EXP. No.	SEC.	$\bar{y} = (y_1 + y_7)/2$	$\bar{y} - y_1 = f(x_1)$	$\bar{y} - y_2 = f(x_2)$	$\bar{y} - y_3 = f(x_3)$	$\bar{y} - y_4 = f(x_4)$	$\bar{y} - y_5 = f(x_5)$	$\bar{y} - y_6 = f(x_6)$	$\bar{y} - y_7 = f(x_7)$
10	2'	1.7635	-0.0335	0.3725	0.9415	1.2235	0.9635	0.3835	0.0335
	3'	1.695	-0.0190	0.4290	1.0450	1.3560	1.0660	0.4100	0.0190
	4'	1.624	-0.0320	0.4330	1.0560	1.3770	1.0940	0.4420	0.0320
	5'	1.5795	-0.0175	0.4655	1.1145	1.4385	1.1345	0.4445	0.0175
	6'	1.5225	-0.0135	0.4655	1.1175	1.4355	1.1285	0.4425	0.0135
	7'	1.4740	-0.0210	0.4670	1.1140	1.4490	1.1440	0.4600	0.0210
	8'	1.3830	-0.0080	0.4230	1.0020	1.3010	1.0220	0.3980	0.0080
	9'	1.2870	-0.0040	0.3910	0.9080	1.1770	0.9260	0.3560	0.0040
	2'	1.6555	-0.0055	0.3455	0.8515	1.1055	0.8515	0.3225	0.0055
11	3'	1.5600	-0.0110	0.3890	0.9260	1.1990	0.9350	0.3680	0.0110
	4'	1.5125	-0.0325	0.3895	0.9485	1.2385	0.9825	0.4085	0.0325
	5'	1.4610	-0.0050	0.4140	1.0000	1.2960	1.0120	0.3820	0.0050
	6'	1.4025	-0.0045	0.4305	1.0005	1.2935	1.0045	0.3965	0.0045
	7'	1.3570	-0.0280	0.4030	1.0080	1.3210	1.0400	0.4240	0.0280
	8'	1.3120	-0.0130	0.3900	0.9350	1.2100	0.9310	0.3570	0.0130
	9'	1.1710	0.0100	0.3450	0.8120	1.0480	0.8060	0.2930	-0.0100
	2'	1.5995	0.0055	0.3435	0.7935	1.0105	0.7725	0.2755	-0.0055
	3'	1.4730	-0.0130	0.3430	0.8350	1.0790	0.8380	0.2150	0.0130
12	4'	1.4085	-0.0015	0.3825	0.8595	1.1075	0.8555	0.3195	0.0015
	5'	1.3570	-0.0160	0.3650	0.8950	1.1610	0.9110	0.3650	0.0160
	6'	1.3100	-0.0100	0.3770	0.9050	1.1700	0.9140	0.3640	0.0100
	7'	1.2665	-0.0185	0.3715	0.9155	1.1965	0.9325	0.3725	0.0185
	8'	1.1880	-0.0070	0.3440	0.8180	1.0580	0.8230	0.3200	0.0070
	9'	1.1250	-0.0050	0.3040	0.7450	0.9790	0.7710	0.3030	0.0050

TABLE 2. Continued

EXP. No.	SEC.	$\bar{y} =$ (y_1+y_7)/2	$\bar{y}-y_1 =$ $f(x_1)$	$\bar{y}-y_2 =$ $f(x_2)$	$\bar{y}-y_3 =$ $f(x_3)$	$\bar{y}-y_4 =$ $f(x_4)$	$\bar{y}-y_5 =$ $f(x_5)$	$\bar{y}-y_6 =$ $f(x_6)$	$\bar{y}-y_7 =$ $f(x_7)$
13	2'	1.4820	-0.0210	0.02720	0.6680	0.8720	0.6800	0.2620	0.0210
	3'	1.3885	-0.0035	0.3135	0.7435	0.9585	0.7465	0.2735	0.0035
	4'	1.3430	-0.0080	0.3120	0.7730	1.0070	0.7830	0.2960	0.0080
	5'	1.2575	-0.0025	0.3285	0.7985	1.0295	0.8015	0.2965	0.0025
	6'	1.2030	-0.0310	0.3030	0.7780	1.0270	0.8210	0.3320	0.0310
	7'	1.1735	-0.0045	0.3335	0.8215	1.0635	0.8345	0.3155	0.0045
	8'	1.0895	0.0045	0.2995	0.7285	0.9295	0.7195	0.2965	-0.0045
	9'	1.0375	-0.0225	0.2835	0.6605	0.8535	0.6635	0.2595	0.0225
	14	2'	1.3590	-0.0240	0.2040	0.5430	0.7240	0.5660	0.2290
3'		1.2430	-0.0070	0.2430	0.6070	0.7850	0.6140	0.2470	0.0070
4'		1.2165	-0.0115	0.2505	0.6505	0.8545	0.6715	0.2555	0.0115
5'		1.149	-0.0450	0.2510	0.6640	0.8890	0.7190	0.3030	0.0450
6'		1.109	-0.0280	0.2600	0.6830	0.9030	0.7090	0.2830	0.0280
7'		1.0425	0.0015	0.2955	0.7025	0.9035	0.6995	0.2565	-0.0015
8'		0.9795	-0.0295	0.2295	0.5955	0.7895	0.6175	0.2495	0.0295
9'		0.8840	0.0130	0.2040	0.5050	0.6690	0.5140	0.1440	-0.0130
15		2'	1.5450	-0.0150	0.2950	0.7160	0.9270	0.7170	0.2790
	3'	1.4475	-0.0255	0.2995	0.7675	1.0055	0.7975	0.3215	0.0255
	4'	1.4030	-0.0080	0.3330	0.8130	1.0570	0.8230	0.3130	0.0080
	5'	1.3580	-0.0040	0.3590	0.8680	1.1200	0.8750	0.3320	0.0040
	6'	1.2935	-0.0315	0.3295	0.8475	1.1225	0.8875	0.3675	0.0315
	7'	1.2450	-0.0050	0.3790	0.8900	1.1400	0.8890	0.3420	0.0050
	8'	1.1725	-0.0325	0.2955	0.7705	1.0145	0.8005	0.3265	0.0325
	9'	1.0675	-0.0065	0.2605	0.6725	0.8865	0.6925	0.2655	0.0065

E.P.M.	Section									
	2'	3'	4'	5'	6'	7'	8'			
1	0.0065	0.0069	0.0077	0.0106	0.0109	0.0103	0.0102			A ft ²
	0.2196	0.2252	0.2367	0.2675	0.2700	0.2646	0.2625			b ft
	0.04519	0.04651	0.05001	0.06059	0.06164	0.06179	0.0591			R ft
	4'	4.5'	5.0'	5.5'	6.0'	6.5'	7.0'	7.5'	8.0'	Section
2	0.0116	0.0140	0.0152	0.0137	0.0157	0.0142	0.0157	0.0145		A ft ²
	0.2808	0.3008	0.3125	0.3008	0.3158	0.3025	0.3142	0.3042		b ft
	0.06285	0.06768	0.07387	0.06942	0.07557	0.07115	0.07597	0.07246		R ft
3			0.0276	0.0271	0.0282	0.0261	0.0277	0.0269	0.0268	A ft ²
			0.4042	0.4005	0.4058	0.3933	0.4017	0.3975	0.3942	b ft
			0.10307	0.10213	0.10498	0.10053	0.10412	0.10220	0.10261	R ft
4			0.0342	0.0330	0.0350	0.0308	0.0329	0.0331	0.0351	A ft ²
			0.4429	0.4358	0.4425	0.4233	0.4325	0.4333	0.4392	b ft
			0.11670	0.11422	0.11912	0.10993	0.11482	0.11517	0.12034	R ft
5			0.0164	0.0155	0.0173	0.0139	0.0154	0.0142	0.0145	A ft ²
			0.3233	0.3156	0.3283	0.3025	0.3125	0.3017	0.2967	b ft
			0.07688	0.07440	0.07976	0.07012	0.07500	0.07165	0.07317	R ft
6			0.0197	0.0196	0.0213	0.0180	0.0198	0.0192	0.0204	A ft ²
			0.3506	0.3506	0.3600	0.3367	0.3472	0.3456	0.3525	b ft
			0.00470	0.00447	0.004950	0.008114	0.008590	0.008403	0.008777	R ft
	2'	3'	4'	5'	6'	7'	8'	9'	10'	Section
7	0.0263	0.0297	0.0312	0.0342	0.0329	0.0340	0.0297	0.0254	0.0263	A ft ²
	0.3908	0.4092	0.4167	0.4252	0.4242	0.4267	0.4067	0.3250	0.3283	b ft
	0.10221	0.10921	0.11254	0.11779	0.11592	0.11712	0.10954	0.09954	0.10192	R ft
8	0.0245	0.0261	0.0277	0.0277	0.0269	0.0272	0.0208			A ft ²
	0.3775	0.3667	0.3458	0.4000	0.3900	0.3850	0.3542			b ft
	0.09796	0.10154	0.10504	0.10833	0.10363	0.10242	0.09700			R ft
9	0.0229	0.0276	0.0282	0.0304	0.0303	0.0306				A ft ²
	0.3717	0.3450	0.4000	0.4108	0.4108	0.4100				b ft
	0.09483	0.10500	0.10600	0.11092	0.11087	0.11179				R ft
10	0.0266	0.0315	0.0325	0.0348	0.0393	0.0352	0.0295	0.0250		A ft ²
	0.3925	0.4183	0.4233	0.4342	0.4342	0.4358	0.4075	0.3817		b ft
	0.10196	0.11300	0.11475	0.11987	0.11962	0.12075	0.10842	0.09808		R ft
11	0.0221	0.0255	0.0271	0.0289	0.0290	0.0298	0.0256	0.0203		A ft ²
	0.3642	0.3825	0.3917	0.4033	0.4033	0.4067	0.3842	0.3517		b ft
	0.09212	0.09992	0.10321	0.10800	0.10779	0.11008	0.10083	0.08733		R ft
12	0.0189	0.0207	0.0222	0.0240	0.0242	0.0251	0.0204	0.0178		A ft ²
	0.3383	0.3542	0.3633	0.3725	0.3725	0.3792	0.3483	0.3292		b ft
	0.08421	0.08992	0.09219	0.09675	0.09750	0.09971	0.08817	0.08158		R ft
13	0.0145	0.0171	0.0185	0.0192	0.0192	0.0204	0.0162	0.0138		A ft ²
	0.3025	0.3225	0.3342	0.3383	0.3367	0.3458	0.3142	0.2908		b ft
	0.07267	0.07987	0.08392	0.08579	0.08558	0.08862	0.07746	0.07112		R ft
14	0.0104	0.0120	0.0139	0.0148	0.0151	0.0152	0.0120	0.0088		A ft ²
	0.2618	0.2767	0.2958	0.3000	0.3033	0.3042	0.2758	0.2458		b ft
	0.06033	0.06542	0.07121	0.07408	0.07525	0.07529	0.06579	0.05575		R ft
15	0.0163	0.0188	0.0205	0.0224	0.0225	0.0231	0.0189	0.0151		A ft ²
	0.3175	0.3375	0.3508	0.3617	0.3625	0.3633	0.3367	0.3108		b ft
	0.07725	0.08379	0.08808	0.09333	0.09354	0.09500	0.08454	0.07387		R ft

TABLE 3.

R^2	$2E$	K	$2E-K$	R/b	A/b^2	W/b	θ_0	$Sec \theta_0$
0.20	2.9780	1.6596	1.3184	0.3392	0.2301	1.259	53° 8'	1.6668
0.18	2.9950	1.6497	1.3453	0.3159	0.2124	1.226	50° 2'	1.5666
0.16	3.0118	1.6400	1.3718	0.2916	0.1948	1.195	47° 10'	1.4709
0.14	3.0286	1.6306	1.3980	0.2675	0.1774	1.166	43° 57'	1.3890
0.12	3.0452	1.6214	1.4238	0.2432	0.1602	1.139	40° 32'	1.3157
0.10	3.0616	1.6124	1.4492	0.2180	0.1428	1.113	36° 53'	1.2502
0.08	3.0778	1.6037	1.4741	0.1920	0.1252	1.088	32° 53'	1.1908

TABLE 4.

	2'	3'	4'	5'	6'	7'	8'			Section
1	0.2058	0.2060	0.2113	0.2265	0.2283	0.2339	0.2250			h-m/b
	0.1345	0.1348	0.1382	0.1486	0.1500	0.1468	0.1478			Am/b ²
	1.1019	1.1020	1.1068	1.122	1.124	1.130	1.121			w-m/b
	4'	4.5'	5.0'	5.5'	6.0'	6.5'	7.0	7.5'	8'	Section
2	0.2238	0.2252	0.2364	0.2308	0.2393	0.2352	0.2418	0.2382		h-m/b
	0.1469	0.1550	0.1560	0.1518	0.1580	0.1550	0.1595	0.1570		Am/b ²
	1.119	1.121	1.132	1.126	1.135	1.131	1.137	1.134		w-m/b
3			0.2550	0.2550	0.2587	0.2556	0.2592	0.2571	0.2603	h-m/b
			0.1688	0.1688	0.1711	0.1689	0.1714	0.1701	0.1726	Am/b ²
			1.152	1.152	1.156	1.152	1.156	1.154	1.158	w-m/b
4			0.2635	0.2621	0.2692	0.2597	0.2655	0.2658	0.2740	h-m/b
			0.1744	0.1738	0.1786	0.1718	0.1760	0.1762	0.1820	Am/b ²
			1.161	1.160	1.168	1.157	1.163	1.164	1.174	w-m/b
5			0.2378	0.2356	0.2430	0.2318	0.2400	0.2375	0.2493	h-m/b
			0.1568	0.1552	0.1605	0.1523	0.1583	0.1565	0.1648	Am/b ²
			1.133	1.131	1.138	1.127	1.136	1.133	1.145	w-m/b
6			0.2422	0.2408	0.2486	0.2410	0.2460	0.2430	0.2490	h-m/b
			0.1600	0.1589	0.1642	0.1590	0.1623	0.1605	0.1647	Am/b ²
			1.138	1.136	1.145	1.137	1.142	1.138	1.145	w-m/b
	2'	3'	4'	5'	6'	7'	8'	9'	10'	Section
7	0.2615	0.2669	0.2701	0.2766	0.2733	0.2745	0.2693	0.2585	0.2625	h-m/b
	0.1722	0.1774	0.1797	0.1886	0.1829	0.1868	0.1796	0.1714	0.1744	Am/b ²
	1.159	1.165	1.169	1.177	1.173	1.174	1.168	1.156	1.160	w-m/b
8	0.2595	0.2626	0.2654	0.2708	0.2662	0.2660	0.2513	0		h-m/b
	0.1719	0.1746	0.1769	0.1800	0.1768	0.1835	0.1659			Am/b ²
	1.157	1.160	1.163	1.169	1.164	1.164	1.147			w-m/b
9	0.2551	0.2658	0.2650	0.2700	0.2699	0.2726				h-m/b
	0.1632	0.1772	0.1764	0.1803	0.1798	0.1821				Am/b ²
	1.152	1.164	1.163	1.168	1.168	1.172				w-m/b
10	0.2598	0.2701	0.2711	0.2761	0.2755	0.2771	0.2661	0.2569		h-m/b
	0.1727	0.1800	0.1814	0.1846	0.1870	0.1854	0.1777	0.1716		Am/b ²
	1.157	1.169	1.170	1.176	1.175	1.177	1.164	1.154		w-m/b
11	0.2529	0.2612	0.2635	0.2678	0.2673	0.2707	0.2624	0.2483		h-m/b
	0.1667	0.1743	0.1767	0.1776	0.1782	0.1802	0.1734	0.1641		Am/b ²
	1.149	1.159	1.161	1.166	1.166	1.170	1.160	1.144		w-m/b
12	0.2489	0.2539	0.2540	0.2597	0.2617	0.2629	0.2531	0.2478		h-m/b
	0.1652	0.1651	0.1682	0.1730	0.1745	0.1745	0.1682	0.1642		Am/b ²
	1.145	1.150	1.151	1.157	1.159	1.161	1.150	1.144		w-m/b
13	0.2402	0.2476	0.2511	0.2536	0.2542	0.2563	0.2465	0.2446		h-m/b
	0.1585	0.1644	0.1656	0.1678	0.1693	0.1706	0.1641	0.1631		Am/b ²
	1.136	1.143	1.147	1.150	1.151	1.153	1.142	1.140		w-m/b
14	0.2304	0.2364	0.2407	0.2469	0.2481	0.2475	0.2385	0.2268		h-m/b
	0.1518	0.1566	0.1588	0.1644	0.1641	0.1643	0.1577	0.1457		Am/b ²
	1.126	1.132	1.136	1.143	1.144	1.143	1.134	1.122		w-m/b
15	0.2433	0.2483	0.2511	0.2580	0.2580	0.2615	0.2511	0.2377		h-m/b
	0.1617	0.1650	0.1665	0.1712	0.1712	0.1750	0.1667	0.1563		Am/b ²
	1.139	1.144	1.147	1.155	1.155	1.159	1.147	1.133		w-m/b

TABLE 5.

Exp. No.	2'	3'	4'	5'	6'	7'	8'			Section			
	1	0.2077	0.2081	0.2132	0.2284	0.2302	0.2360	0.2271			h c / b		
0.1359		0.1365	0.1386	0.1492	0.1506	0.1483	0.1492			Ac / b ²			
1.221		1.249	1.233	1.272	1.278	1.290	1.270			Sec 00			
2	4'	4.5'	5.0'	5.5'	6.0'	6.5'	7.0'	7.5'	8.0'	Section			
	0.2256	0.2267	0.2382	0.2326	0.2411	0.2371	0.2437	0.2401			h c / b		
	0.1482	0.1556	0.1566	0.1524	0.1585	0.1562	0.1600	0.1578			Ac / b ²		
3	1.266	1.270	1.299	1.283	1.305	1.295	1.311	1.302			Sec 00		
			0.2566	0.2566	0.2604	0.2573	0.2609	0.2588	0.2621			h c / b	
			0.1695	0.1696	0.1724	0.1694	0.1729	0.1707	0.1737			Ac / b ²	
4			1.350	1.350	1.361	1.352	1.364	1.358	1.368			Sec 00	
			0.2651	0.2637	0.2709	0.2613	0.2672	0.2675	0.2752			h c / b	
			0.1753	0.1747	0.1796	0.1728	0.1769	0.1771	0.1830			Ac / b ²	
5			1.378	1.372	1.395	1.365	1.383	1.384	1.411			Sec 00	
			0.2396	0.2374	0.2449	0.2336	0.2419	0.2394	0.2515			h c / b	
			0.1579	0.1565	0.1615	0.1529	0.1588	0.1570	0.1660			Ac / b ²	
6			1.301	1.297	1.317	1.288	1.309	1.300	1.335			Sec 00	
			0.2431	0.2425	0.2504	0.2427	0.2478	0.2448	0.2508			h c / b	
			0.1610	0.1599	0.1652	0.1600	0.1632	0.1614	0.1657			Ac / b ²	
7			1.312	1.310	1.331	1.310	1.324	1.317	1.332			Sec 00	
	2'	3'	4'	5'	6'	7'	8'	9'	10'	Section			
	0.2633	0.2687	0.2719	0.2785	0.2751	0.2763	0.2712	0.2603	0.2643			h c / b	
8	0.1729	0.1786	0.1809	0.1898	0.1841	0.1880	0.1808	0.1721	0.1756			Ac / b ²	
	1.370	1.388	1.400	1.470	1.410	1.413	1.395	1.361	1.375			Sec 00	
	0.2613	0.2644	0.2672	0.2728	0.2681	0.2679	0.2531					h c / b	
9	0.1726	0.1752	0.1782	0.1812	0.1782	0.1849	0.1667					Ac / b ²	
	1.365	1.375	1.383	1.410	1.388	1.385	1.340					Sec 00	
	0.2569	0.2601	0.2668	0.2719	0.2718	0.2746							h c / b
10	0.1635	0.1782	0.1775	0.1814	0.1808	0.1832							Ac / b ²
	1.351	1.384	1.381	1.399	1.399	1.408							Sec 00
	0.2615	0.2720	0.2729	0.2779	0.2773	0.2789	0.2679	0.2587					h c / b
11	0.1734	0.1811	0.1825	0.1857	0.1880	0.1864	0.1789	0.1723					Ac / b ²
	1.159	1.171	1.172	1.178	1.177	1.180	1.166	1.156					Sec 00
	0.2547	0.2631	0.2653	0.2696	0.2691	0.2725	0.2643	0.2501					h c / b
12	0.1674	0.1777	0.1806	0.1813	0.1812	0.1838	0.1775	0.1681					Ac / b ²
	1.344	1.370	1.378	1.391	1.389	1.400	1.374	1.332					Sec 00
	0.2508	0.2557	0.2559	0.2616	0.2636	0.2648	0.2550	0.2497					h c / b
13	0.1661	0.1659	0.1689	0.1737	0.1752	0.1752	0.1690	0.1651					Ac / b ²
	1.332	1.348	1.349	1.367	1.370	1.376	1.346	1.330					Sec 00
	0.2422	0.2496	0.2530	0.2556	0.2562	0.2582	0.2485	0.2467					h c / b
14	0.1596	0.1654	0.1665	0.1687	0.1702	0.1714	0.1651	0.1643					Ac / b ²
	1.308	1.329	1.340	1.347	1.350	1.355	1.326	1.320					Sec 00
	0.2322	0.2385	0.2427	0.2490	0.2502	0.2496	0.2406	0.2289					h c / b
15	0.1533	0.1520	0.1600	0.1655	0.1652	0.1654	0.1590	0.1473					Ac / b ²
	1.283	1.300	1.310	1.327	1.330	1.329	1.303	1.272					Sec 00
	0.2452	0.2501	0.2529	0.2599	0.2599	0.2634	0.2530	0.2595					h c / b
15	0.1627	0.1659	0.1673	0.1720	0.1720	0.1757	0.1675	0.1573					Ac / b ²
	1.317	1.331	1.340	1.360	1.360	1.370	1.340	1.301					Sec 00

TABLE 6.

EXP. NO.

	2'	3'	4'	5'	6'	7'	8'			Section
1	0.04519	0.04651	0.05001	0.06059	0.06164	0.06189	0.05910			R (ft)
	0.07440	0.07280	0.07200	0.06600	0.06500	0.06610	0.06720			Z (ft)
	0.11959	0.11931	0.12201	0.12659	0.12664	0.12719	0.12630			H (ft)
	4.0'	4.5'	5.0'	5.5'	6.0'	6.5'	7.0'	7.5'	8.0'	Section
2	0.06285	0.06768	0.07387	0.06942	0.07557	0.07115	0.07597	0.07246		R (ft)
	0.05430	0.05080	0.04800	0.05020	0.04690	0.05200	0.04880	0.05220		Z (ft)
	0.11715	0.11848	0.12187	0.11962	0.12247	0.12315	0.12477	0.12466		H (ft)
3			0.10307	0.10213	0.10498	0.10053	0.10412	0.10220	0.10261	R (ft)
			0.02830	0.02970	0.02610	0.03180	0.02930	0.03190	0.03250	Z (ft)
			0.13137	0.13183	0.13108	0.13233	0.13342	0.13410	0.13511	H (ft)
4			0.11670	0.11422	0.11912	0.10993	0.11482	0.11517	0.12034	R (ft)
			0.02450	0.02610	0.0226	0.0284	0.02570	0.02810	0.03040	Z (ft)
			0.14120	0.14032	0.14172	0.13833	0.14052	0.14327	0.15074	H (ft)
5			0.07688	0.07440	0.07978	0.07012	0.07500	0.07165	0.07397	R (ft)
			0.03360	0.03590	0.03320	0.03720	0.03630	0.03990	0.04190	Z (ft)
			0.11048	0.11030	0.11298	0.10932	0.11130	0.11155	0.11587	H (ft)
6			0.08470	0.08447	0.08950	0.08114	0.08590	0.08403	0.08777	R (ft)
			0.03330	0.03530	0.03180	0.03700	0.03520	0.03750	0.03650	Z (ft)
			0.11800	0.11977	0.12130	0.11814	0.11810	0.12153	0.12427	H (ft)
	2'	3'	4'	5'	6'	7'	8'	9'	10'	Section
7	0.10221	0.10921	0.11254	0.11779	0.11592	0.11712	0.10754	0.09954	0.10192	R (ft)
	0.04367	0.03611	0.03397	0.02915	0.03002	0.02930	0.04050	0.04764	0.04823	Z (ft)
	0.14588	0.14532	0.14651	0.14774	0.14594	0.14642	0.15004	0.14918	0.15015	H (ft)
8	0.09790	0.10154	0.10504	0.10833	0.10383	0.10242	0.08900			R (ft)
	0.04408	0.03980	0.03932	0.03764	0.04066	0.04310	0.05408			Z (ft)
	0.14204	0.14134	0.14436	0.14597	0.14449	0.14552	0.14308			H (ft)
9	0.09483	0.10500	0.10600	0.11092	0.11087	0.11179				R (ft)
	0.04650	0.03974	0.03817	0.03529	0.03473	0.03522				Z (ft)
	0.14133	0.14494	0.14417	0.14621	0.14560	0.14701				H (ft)
10	0.10196	0.11300	0.11475	0.11987	0.11962	0.12075	0.10842	0.09808		R (ft)
	0.04500	0.03698	0.03484	0.03183	0.03198	0.03205	0.04320	0.05281		Z (ft)
	0.14696	0.14998	0.14959	0.15170	0.15160	0.15280	0.15162	0.15089		H (ft)
11	0.09212	0.09992	0.10321	0.10800	0.10779	0.11008	0.10083	0.08733		R (ft)
	0.04583	0.03000	0.02783	0.031375	0.03008	0.03000	0.00850	0.01025		Z (ft)
	0.13795	0.13873	0.14001	0.14067	0.14059	0.14160	0.14425	0.13942		H (ft)
12	0.08421	0.08992	0.09229	0.09675	0.09750	0.09971	0.08817	0.08158		R (ft)
	0.04908	0.04156	0.03876	0.03437	0.03436	0.03347	0.04443	0.05252		Z (ft)
	0.13329	0.13148	0.13105	0.13112	0.13186	0.13318	0.13260	0.13410		H (ft)
13	0.07267	0.07987	0.08392	0.08579	0.08558	0.08862	0.07746	0.07112		R (ft)
	0.05083	0.04427	0.04139	0.03675	0.03678	0.03623	0.04650	0.05548		Z (ft)
	0.12350	0.12414	0.12531	0.12254	0.12236	0.12485	0.12396	0.12660		H (ft)
14	0.06033	0.06542	0.07121	0.07408	0.07525	0.07529	0.06579	0.05575		R (ft)
	0.05292	0.04646	0.04341	0.03898	0.03913	0.03849	0.04856	0.05763		Z (ft)
	0.11325	0.11188	0.11462	0.11306	0.11438	0.11378	0.11435	0.11338		H (ft)
15	0.07725	0.08379	0.08808	0.09333	0.09354	0.09500	0.08454	0.07387		R (ft)
	0.05150	0.04527	0.04207	0.03772	0.03635	0.03521	0.04545	0.05434		Z (ft)
	0.12875	0.12906	0.13015	0.13005	0.12989	0.13021	0.12999	0.12821		H (ft)

TABLE 7.

TABLE 8.

EXP. NO.	Wc	R _{mean}	A ³ × 10 ⁶	$\frac{Q}{ft^3/sec.}$	$\frac{D \times 10^5}{ft^2/sec.}$	$\frac{-a.k.z_i}{\times 10^5}$	R \bar{C}	C \bar{F}	S _a × 10 ⁵	t _{0.5} × S _a × 10 ⁵	Prob. error × 10 ⁵	% error
1	0.2790	1635	0.7490	0.0052	1.14	152.18	15.92	0.00974	32.80	23.80	±2.49	15.64
2	0.3439	2375	2.998	0.0093	1.14	216.68	33.32	0.01463	8.80	6.32	±0.97	2.92
3	0.4620	3643	20.43	0.0192	1.14	129.28	36.44	0.01000	11.52	8.37	±2.36	6.48
4	0.5079	4700	38.00	0.0272	1.14	239.72	73.32	0.01560	64.30	46.70	±14.28	19.50
5	0.3542	2922	3.659	0.0118	1.14	126.92	17.73	0.00607	34.40	25.00	±3.49	19.69
6	0.4004	3111	7.800	0.0147	1.18	159.14	28.80	0.00926	28.40	20.65	±3.74	12.99
7	0.4772	2647	27.27	0.0144	1.14	57.03	26.80	0.01012	1.40	1.00	±0.47	1.70
8	0.4535	2964	19.68	0.0151	1.14	82.28	29.45	0.00993	29.50	21.80	±7.80	26.50
9	0.4660	2378	22.90	0.0133	1.20	94.57	40.25	0.01692	27.00	20.00	±8.51	21.10
10	0.4868	2619	32.77	0.0153	1.20	53.64	26.02	0.00993	21.35	15.33	±7.44	28.60
11	0.4484	2224	18.61	0.0118	1.18	51.26	21.94	0.00986	25.00	17.95	±7.68	35.00
12	0.4135	1832	10.30	0.0089	1.18	21.95	8.07	0.00440	16.24	11.66	±4.29	53.00
13	0.3709	1364	5.322	0.0060	1.18	23.12	8.17	0.00599	21.50	15.44	±5.46	66.80
14	0.3219	935	2.147	0.0035	1.18	15.09	4.81	0.00514	14.13	10.14	±3.20	66.50
15	0.3999	1611	8.550	0.0077	1.20	21.71	8.06	0.00500	13.22	9.61	±3.57	44.30

TABLE 9.

d	P	P
0.00	0.0000	0.5000
0.20	0.1590	0.4205
0.40	0.3110	0.3445
0.60	0.4510	0.2745
0.80	0.5760	0.2120
1.00	0.6830	0.1585
1.20	0.7700	0.1150
1.40	0.8380	0.0810
1.60	0.8900	0.0550
1.80	0.9280	0.0360
2.00	0.9540	0.0230
2.20	0.9720	0.0140
2.40	0.9840	0.0080
2.60	0.9910	0.0045
2.80	0.9950	0.0025
3.00	0.9973	0.00135
3.20	0.9986	0.00070
3.40	0.9993	0.00035
3.60	0.9997	0.00015
3.80	0.9999	0.00005

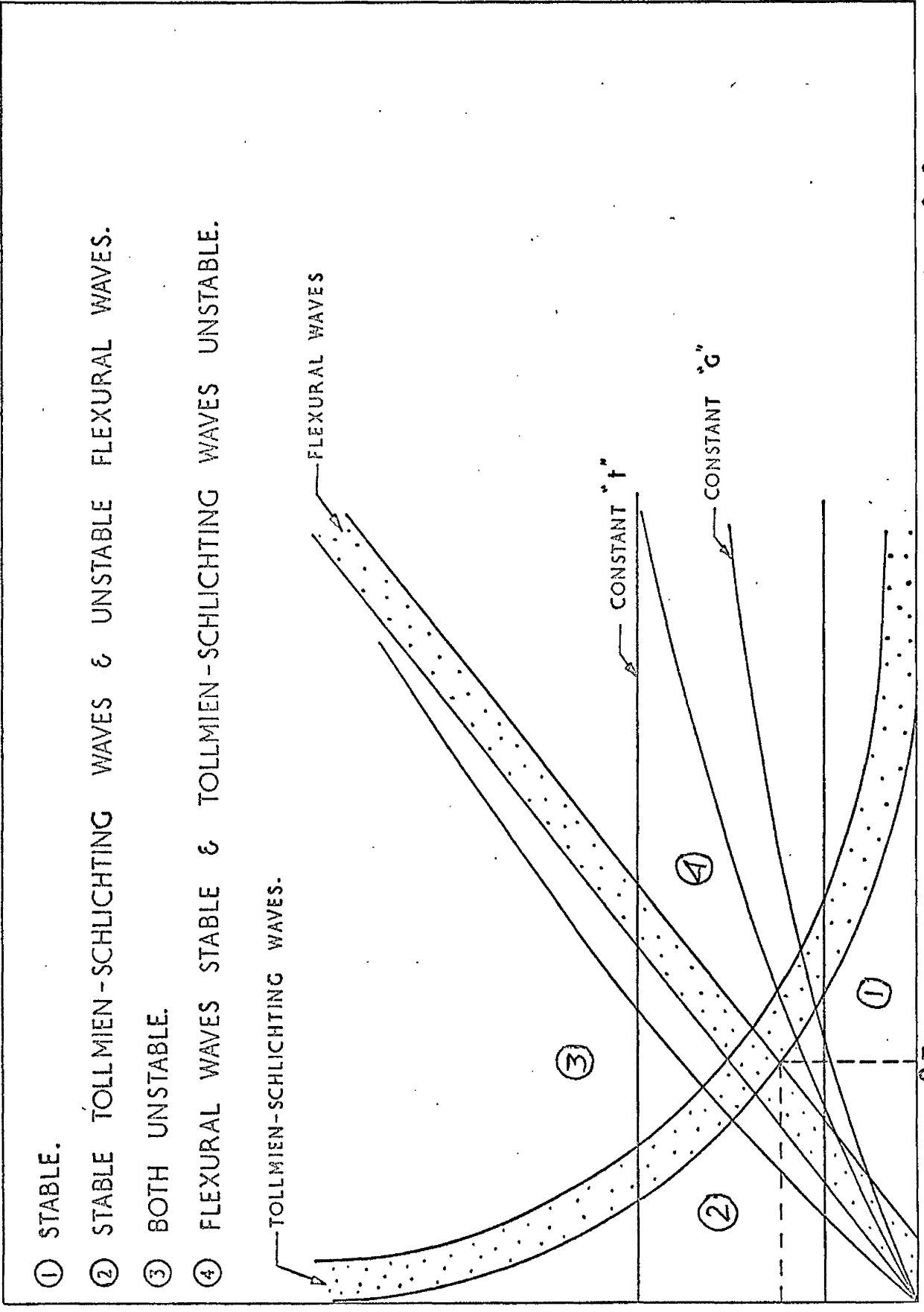
$$P = (1 - P) / 2$$

$P^1(7,8)$	P_{17}	$P(6,7)$	0.0000	$P(7,8)$	0.0000
$P^1(6,8)$	P_{27}	$P(6,7)$	0.0000	$P(6,8)$	0.0000
$P^1(5,8)$	P_{27}	$P(5,7)$	0.0000	$P(5,8)$	0.0000
$P^1(4,8)$	P_{27}	$P(4,7)$	0.0000	$P(4,8)$	0.0000
$P^1(3,8)$	P_{27}	$P(3,7)$	0.0000	$P(3,8)$	0.0000
$P^1(2,8)$	P_{27}	$P(2,7)$	0.0000	$P(2,8)$	0.0000
$P^1(1,8)$	P_{27}	$P(1,7)$	0.0000	$P(1,8)$	0.0000
$P^1(0,8)$	P_{27}	$P(0,7)$	0.0000	$P(0,8)$	0.0000
$P^1(6,7)$	P_{37}	$P(6,7)$	0.0000012	$P(6,7)$	0.0000012
$P^1(5,7)$	P_{37}	$P(5,7)$	0.0000175	$P(5,7)$	0.0000175
$P^1(4,7)$	P_{37}	$P(4,7)$	0.0000400	$P(4,7)$	0.0000400
$P^1(3,7)$	P_{37}	$P(3,7)$	0.0474009	$P(3,7)$	0.0474009
$P^1(2,7)$	P_{37}	$P(2,7)$	0.1406867	$P(2,7)$	0.1406867
$P^1(1,7)$	P_{37}	$P(1,7)$	0.1838336	$P(1,7)$	0.1838336
$P^1(0,7)$	P_{37}	$P(0,7)$	0.1790306	$P(0,7)$	0.1790306
$P^1(5,6)$	P_{37}	$P(5,6)$	0.0000112	$P(5,6)$	0.0000112
$P^1(4,6)$	P_{37}	$P(4,6)$	0.0000250	$P(4,6)$	0.0000250
$P^1(3,6)$	P_{37}	$P(3,6)$	0.0291882	$P(3,6)$	0.0291882
$P^1(2,6)$	P_{37}	$P(2,6)$	0.0866316	$P(2,6)$	0.0866316
$P^1(1,6)$	P_{37}	$P(1,6)$	0.1132007	$P(1,6)$	0.1132007
$P^1(0,6)$	P_{37}	$P(0,6)$	0.1102423	$P(0,6)$	0.1102423
$P^1(4,5)$	P_{37}	$P(4,5)$	0.0000050	$P(4,5)$	0.0000050
$P^1(3,5)$	P_{37}	$P(3,5)$	0.0059224	$P(3,5)$	0.0059224
$P^1(2,5)$	P_{37}	$P(2,5)$	0.0175796	$P(2,5)$	0.0175796
$P^1(1,5)$	P_{37}	$P(1,5)$	0.0229710	$P(1,5)$	0.0229710
$P^1(0,5)$	P_{37}	$P(0,5)$	0.0223708	$P(0,5)$	0.0223708
$P^1(3,4)$	P_{37}	$P(3,4)$	0.0027505	$P(3,4)$	0.0027505
$P^1(2,4)$	P_{37}	$P(2,4)$	0.0081663	$P(2,4)$	0.0081663
$P^1(1,4)$	P_{37}	$P(1,4)$	0.0106704	$P(1,4)$	0.0106704
$P^1(0,4)$	P_{37}	$P(0,4)$	0.0103915	$P(0,4)$	0.0103915
$P^1(2,3)$	P_{37}	$P(2,3)$	0.0016460	$P(2,3)$	0.0016460
$P^1(1,3)$	P_{37}	$P(1,3)$	0.0021513	$P(1,3)$	0.0021513
$P^1(0,3)$	P_{37}	$P(0,3)$	0.0017548	$P(0,3)$	0.0017548
$P^1(1,2)$	P_{37}	$P(1,2)$	0.0014146	$P(1,2)$	0.0014146
$P^1(0,2)$	P_{37}	$P(0,2)$	0.0013796	$P(0,2)$	0.0013796
$P^1(0,1)$	P_{37}	$P(0,1)$	0.0005716	$P(0,1)$	0.0005716

$\Sigma\Sigma$

1.0000000

TABLE II.



$$Gt^2 / \frac{1}{2} P V m^2$$

$$\epsilon$$

$$C_4 / u \delta$$

FIG. 1

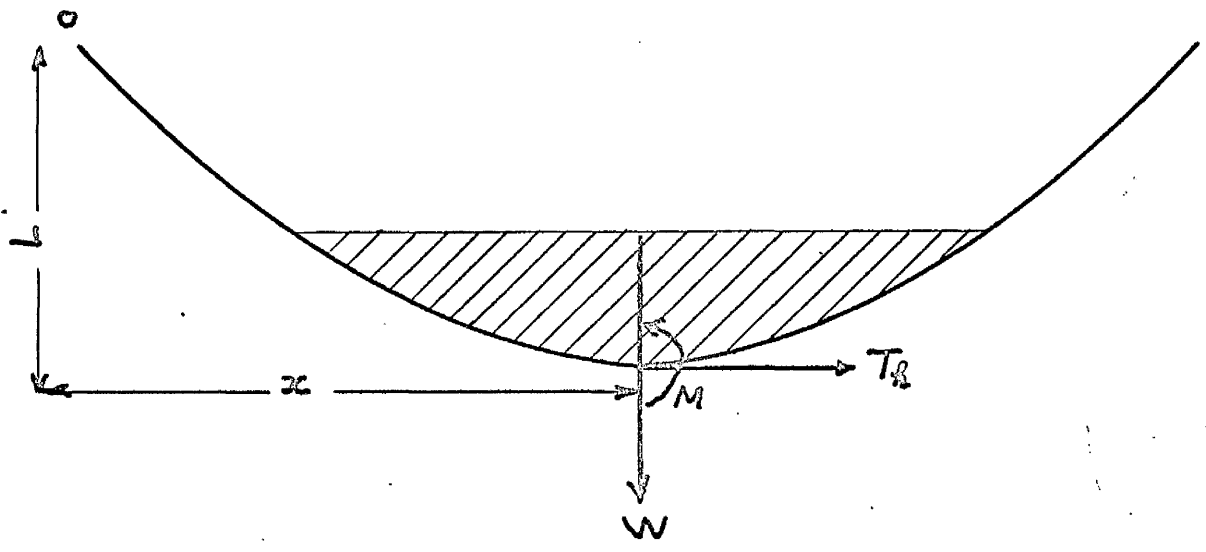


FIG. 2

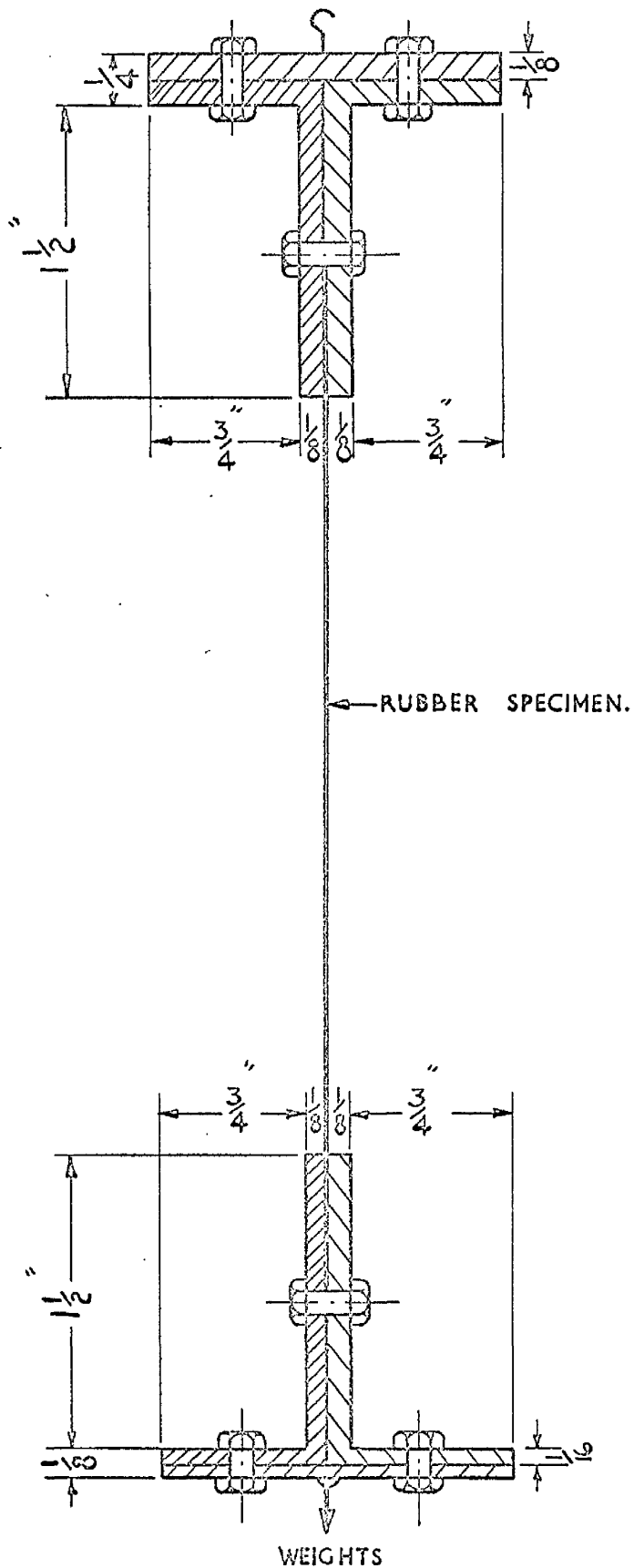
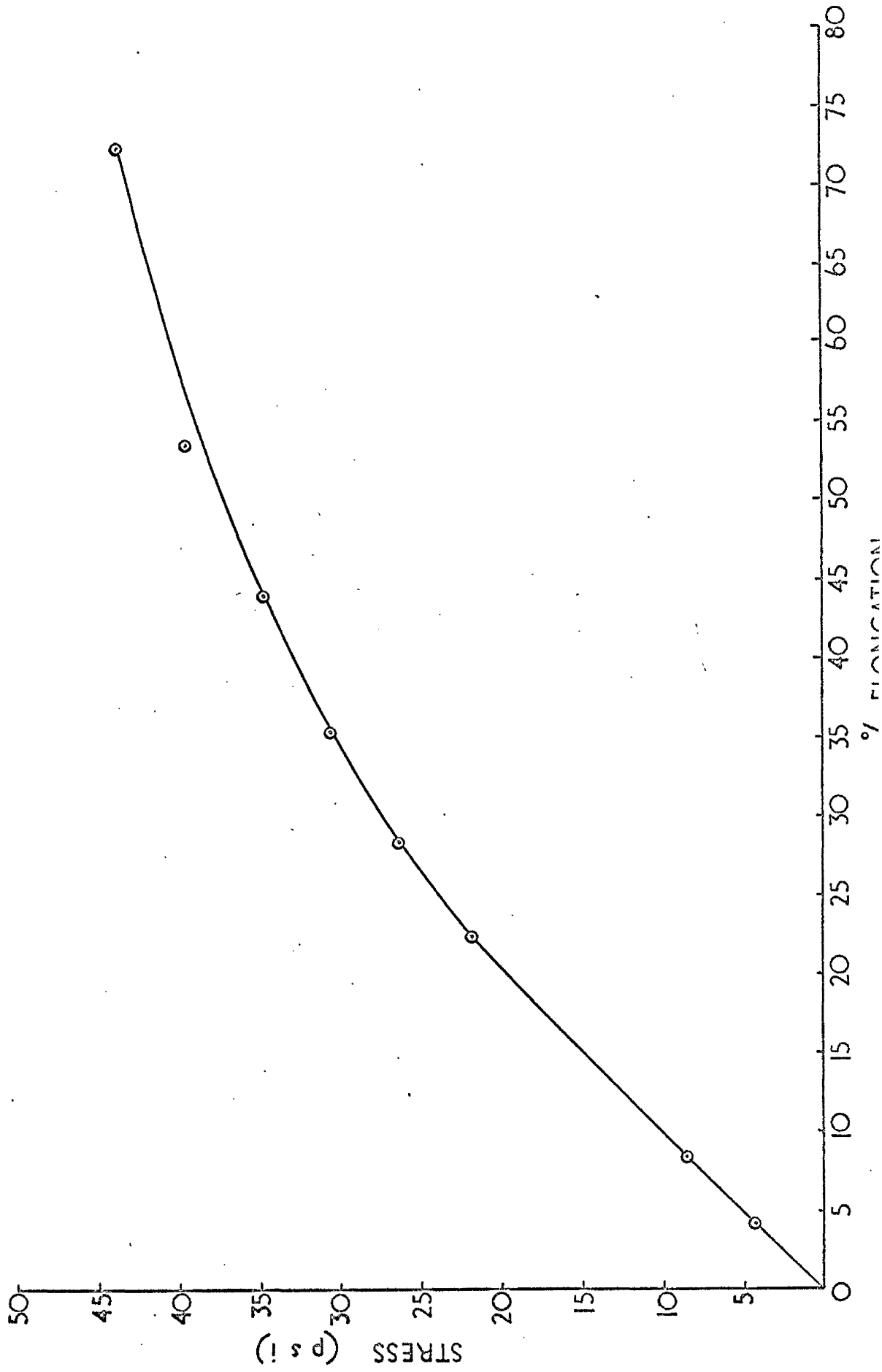


FIG. 3

RUBBER SPECIMEN BETWEEN CLAMPS.

FIG. 4 (d)

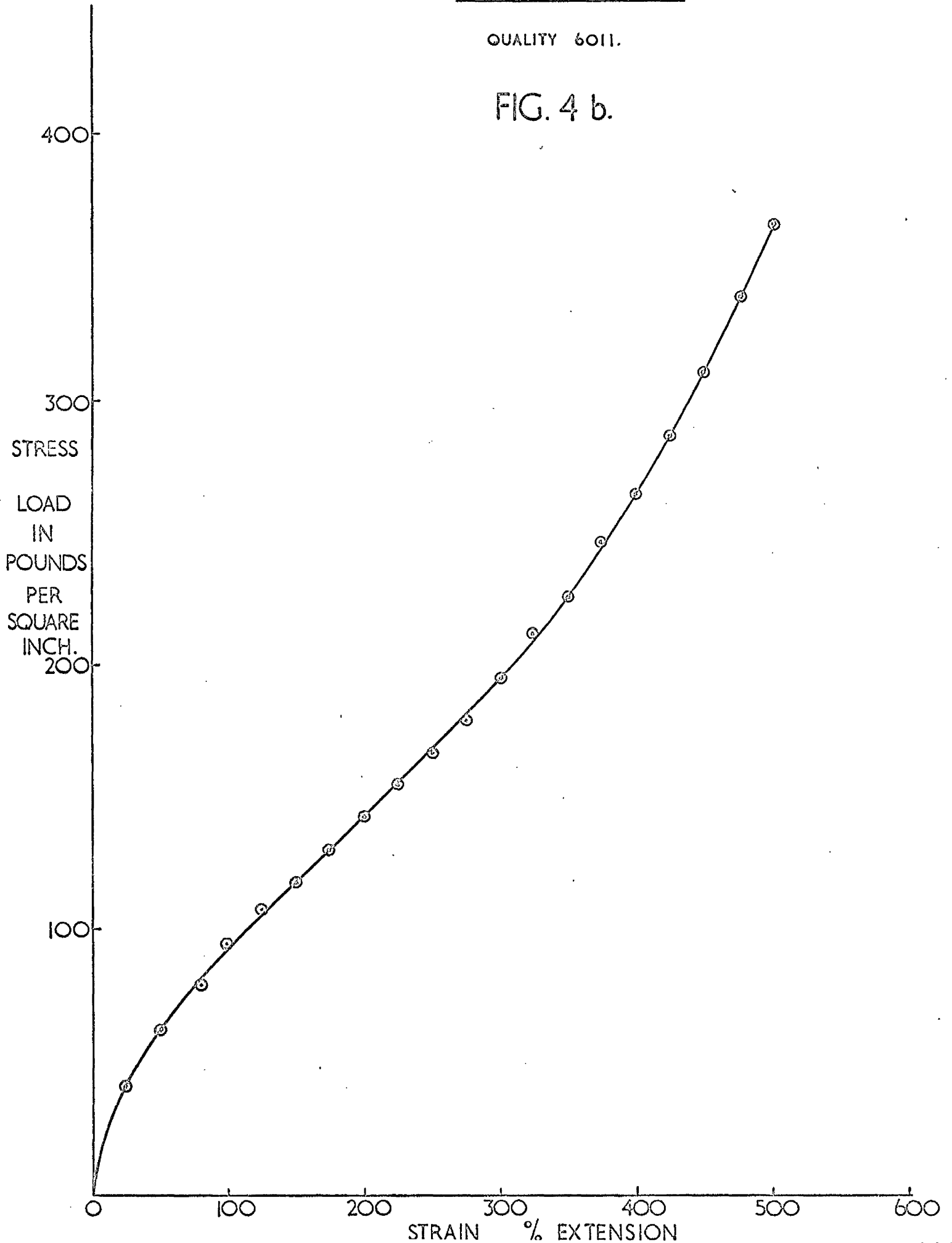
STRESS STRAIN CURVE FOR VULCANISED RUBBER.



STRESS vs STRAIN.

QUALITY 6011.

FIG. 4 b.



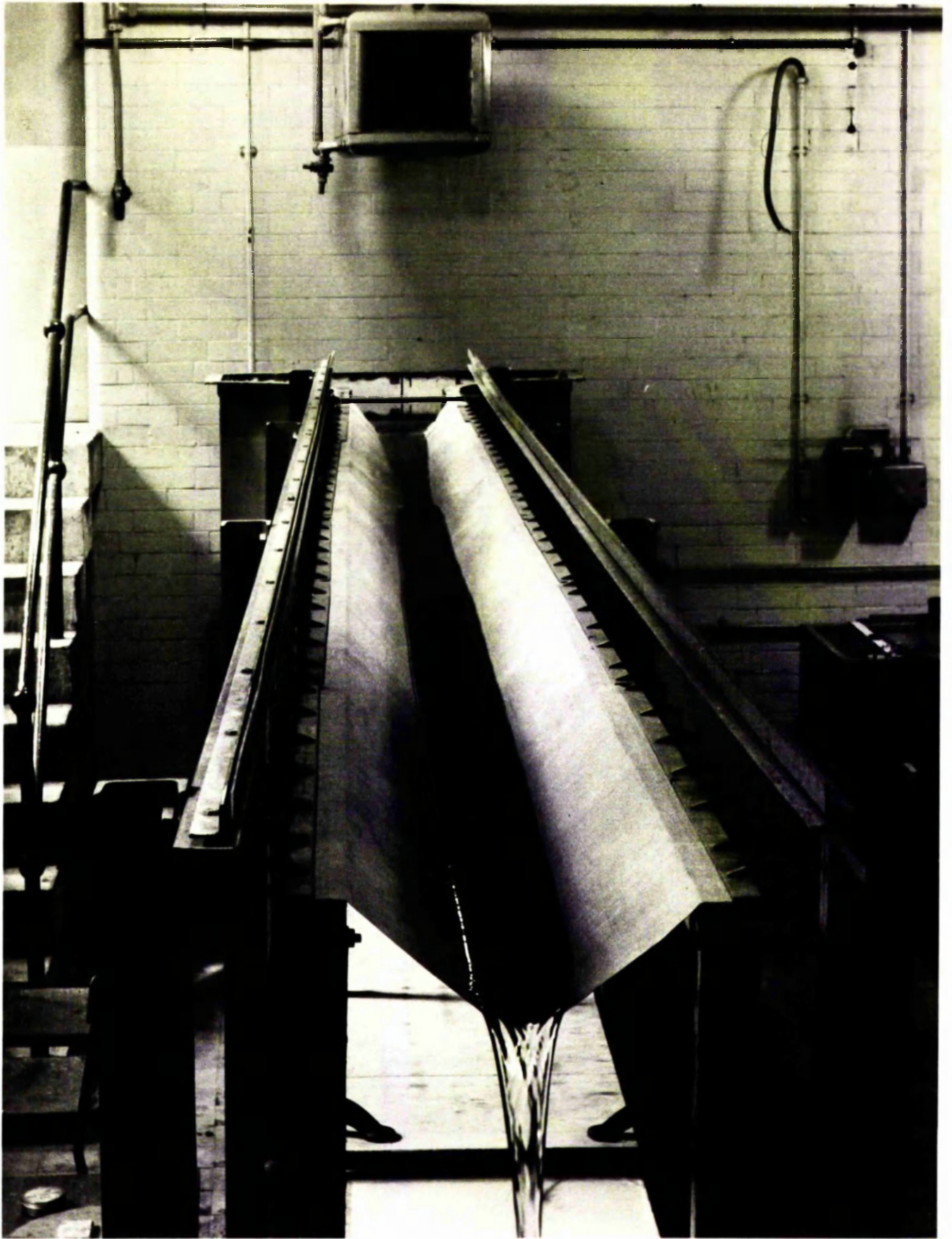


FIG. 5

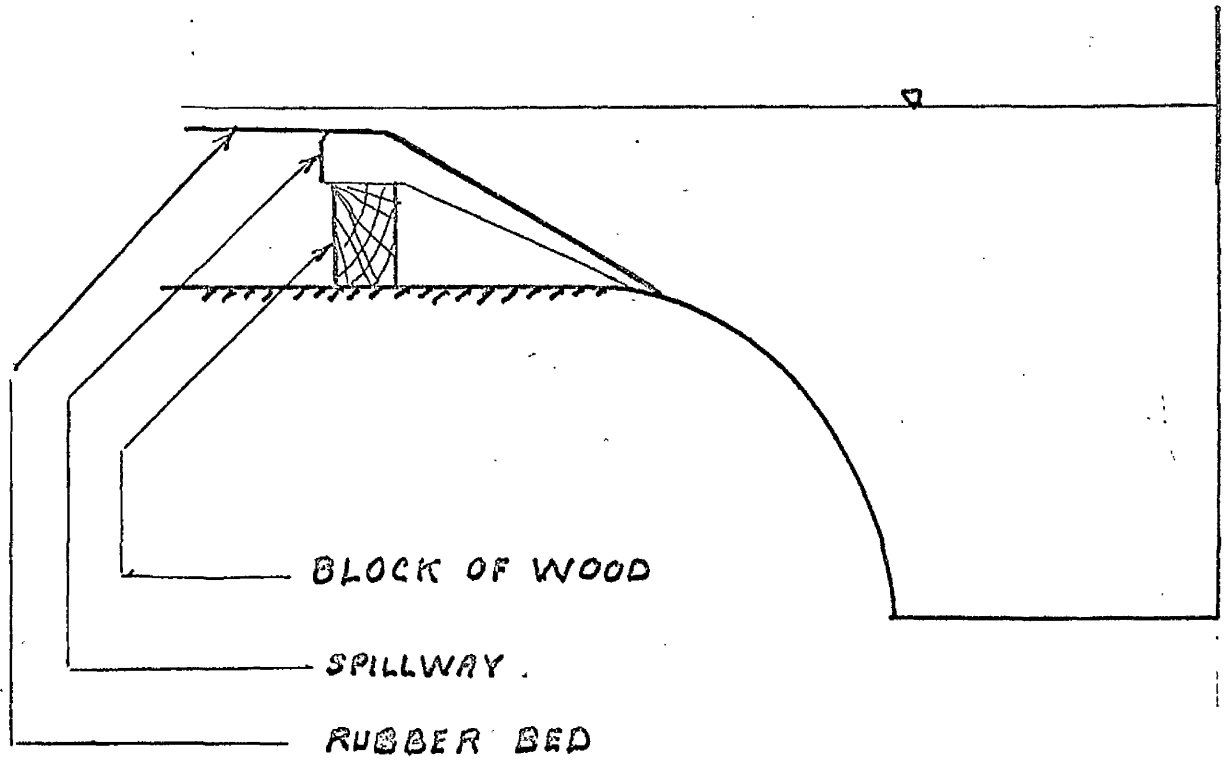
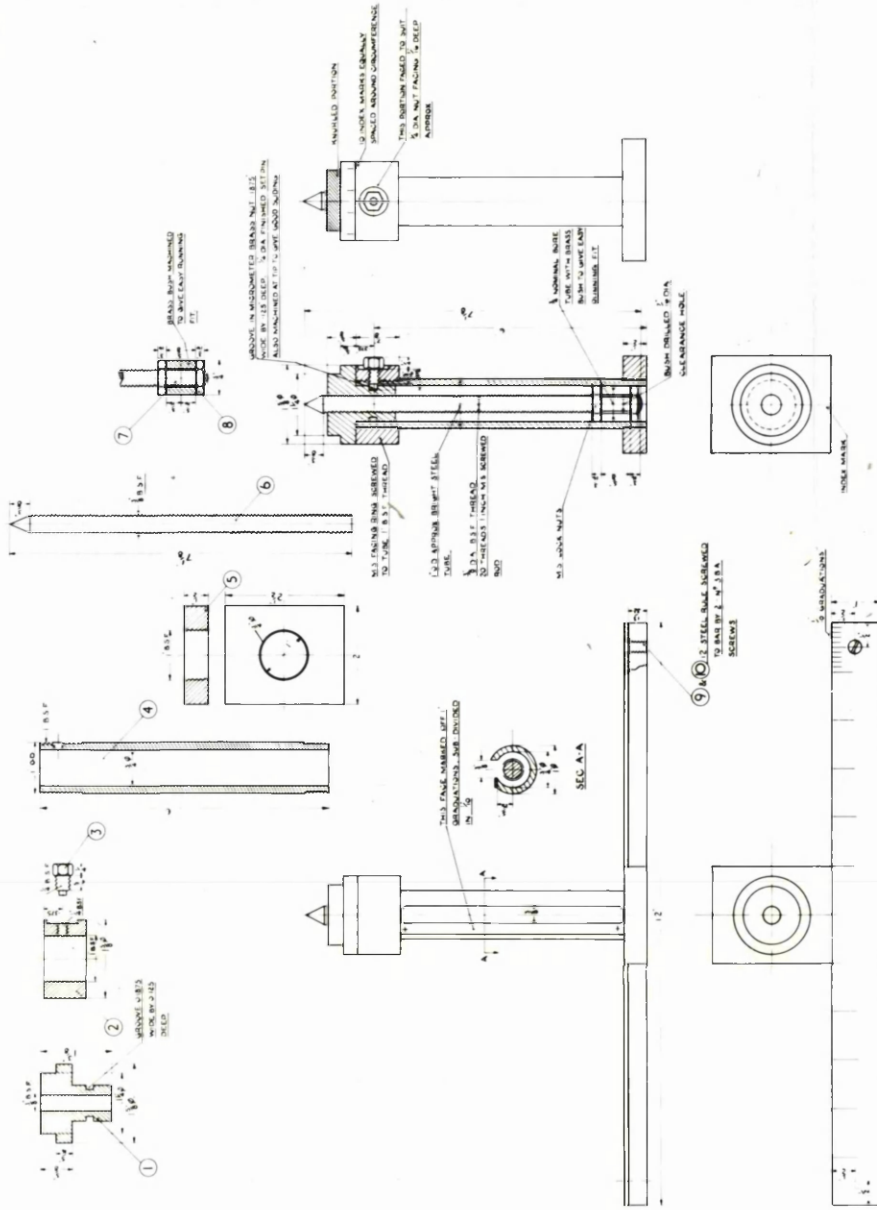


FIG. 6



FIG. 7

DO NOT SCALE DRAWING
IF IN DOUBT—ASK.



SCALE
ITEMS 1, 2, 3, 7, 11 UNDIMENSIONED AND OVER

ITEM No.	DESCRIPTION	MATERIAL	REMARKS
1	BASE	BRASS	
2	FRAME	BRASS	
3	SPINDLE	STEEL	
4	SLIDE	STEEL	
5	THIMBLE	BRASS	
6	STOP	BRASS	
7	SPINDLE	STEEL	
8	SPINDLE NUT	BRASS	

UNIVERSITY OF GLASGOW
ENGINEERING LABORATORIES
TITLE OF DRAWING—MICROMETER HEIGHT GAUGE
TITLE OF PROJECT—CHANNEL FLOW INVESTIGATIONS
DEPARTMENT—AERONAUTICS & FLUID MECHANICS
PROJECT No. _____ SCALE: FULL SIZE
DRAWN BY _____ CHECKED BY _____
APPROVED BY _____ DATE DRAWN: 2. 9. 42. No. OF SHEETS: 31

NOTE: THIS DRAWING IS PRIVATE AND CONFIDENTIAL COMMUNICATION AND THE REPRODUCTION OR DISSEMINATION OF THIS DRAWING WITHOUT THE WRITTEN CONSENT OF THE UNIVERSITY AND MUST BE RETURNED IMMEDIATELY ON COMPLETION OF THE WORK FOR WHICH IT WAS DRAWN.

REVISIONS:

NO.	DESCRIPTION	DATE
1	AS DRAWN	

Fig. 8

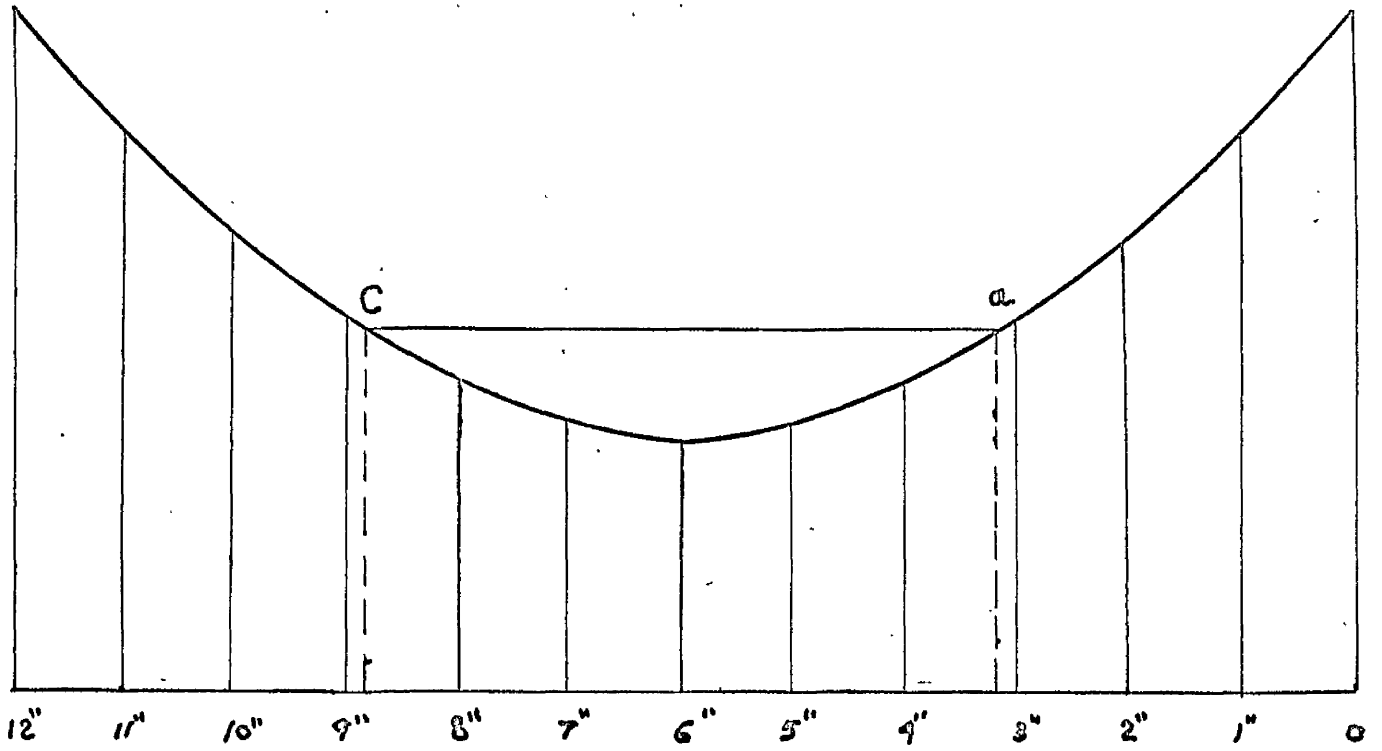


FIG. 9.

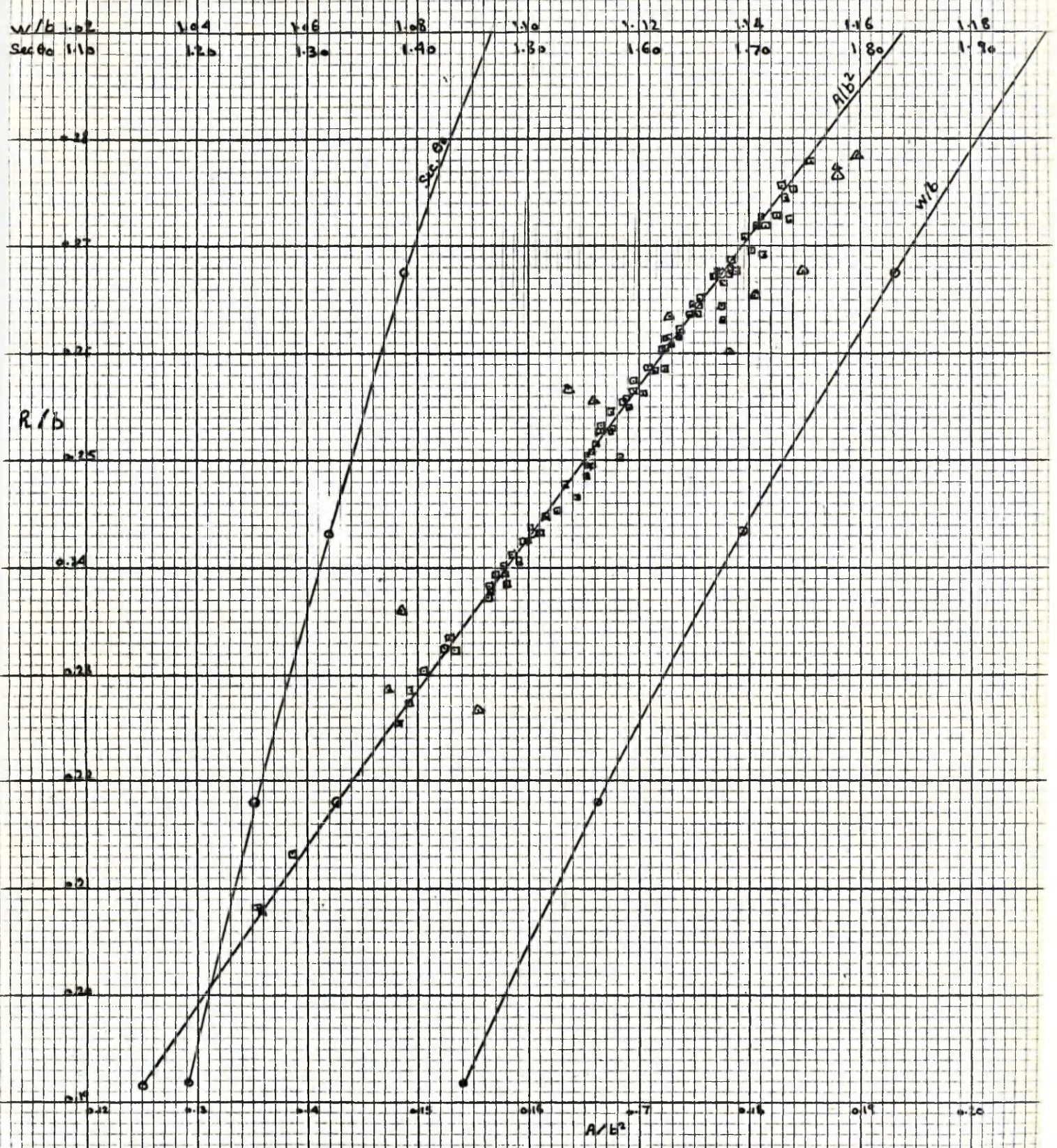


FIG 10

FIG. 11

$P(\omega, \mu)$

6					0.0	
5					0.0	0.0
4				0.0	0.0	0.0
3		0.085	0.000	0.006	0.029	0.047
2		0.390	0.155	0.002	0.017	0.087
1	0.571	0.553	0.001	0.002	0.011	0.025
0	0.324	0.497	0.001	0.002	0.010	0.012
			0.002	0.006	0.032	0.068
			0.002	0.008	0.040	0.08

μ
MATRIX FORM

P (PROBABILITY OF STATE OF FLOW)

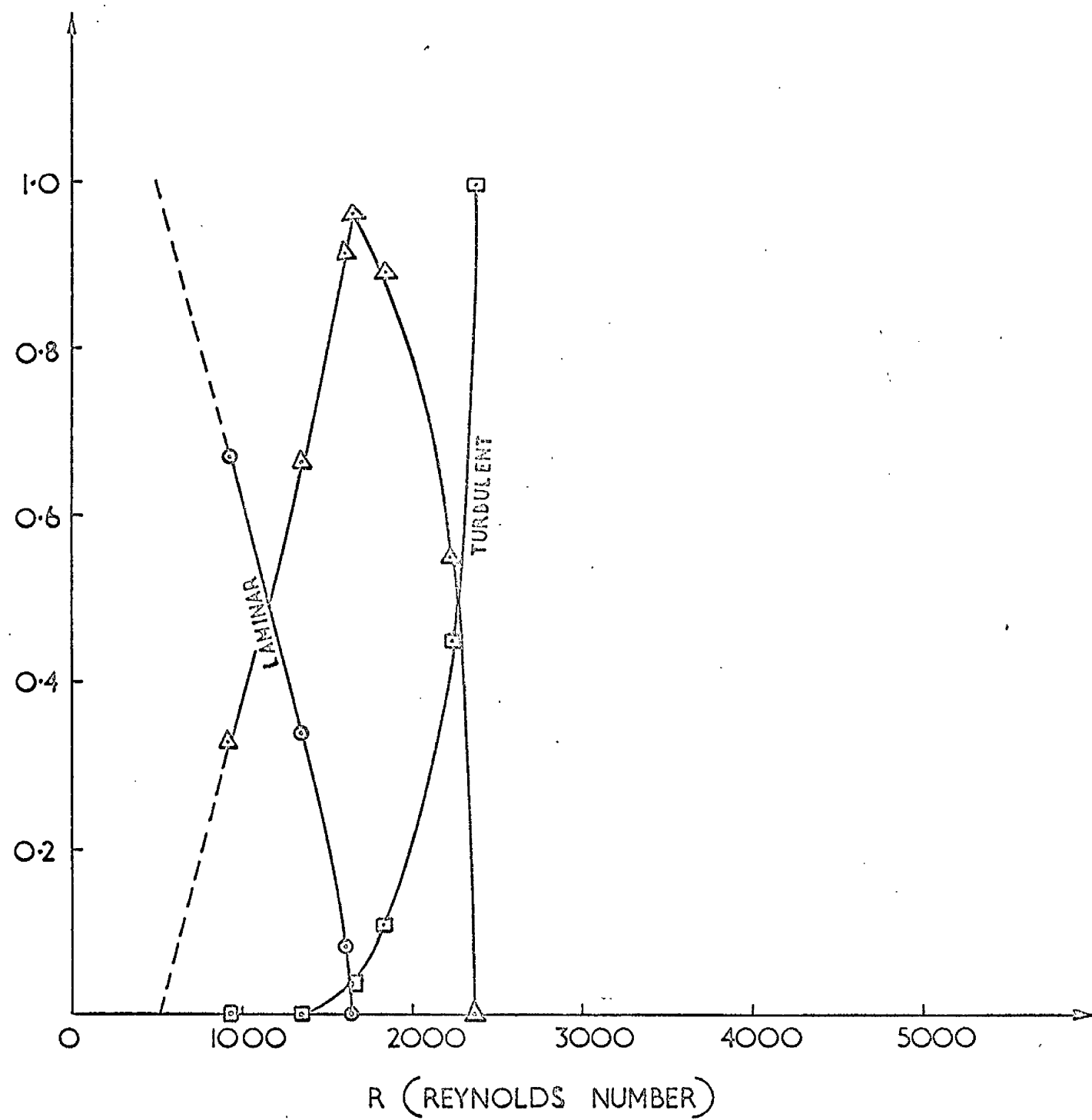
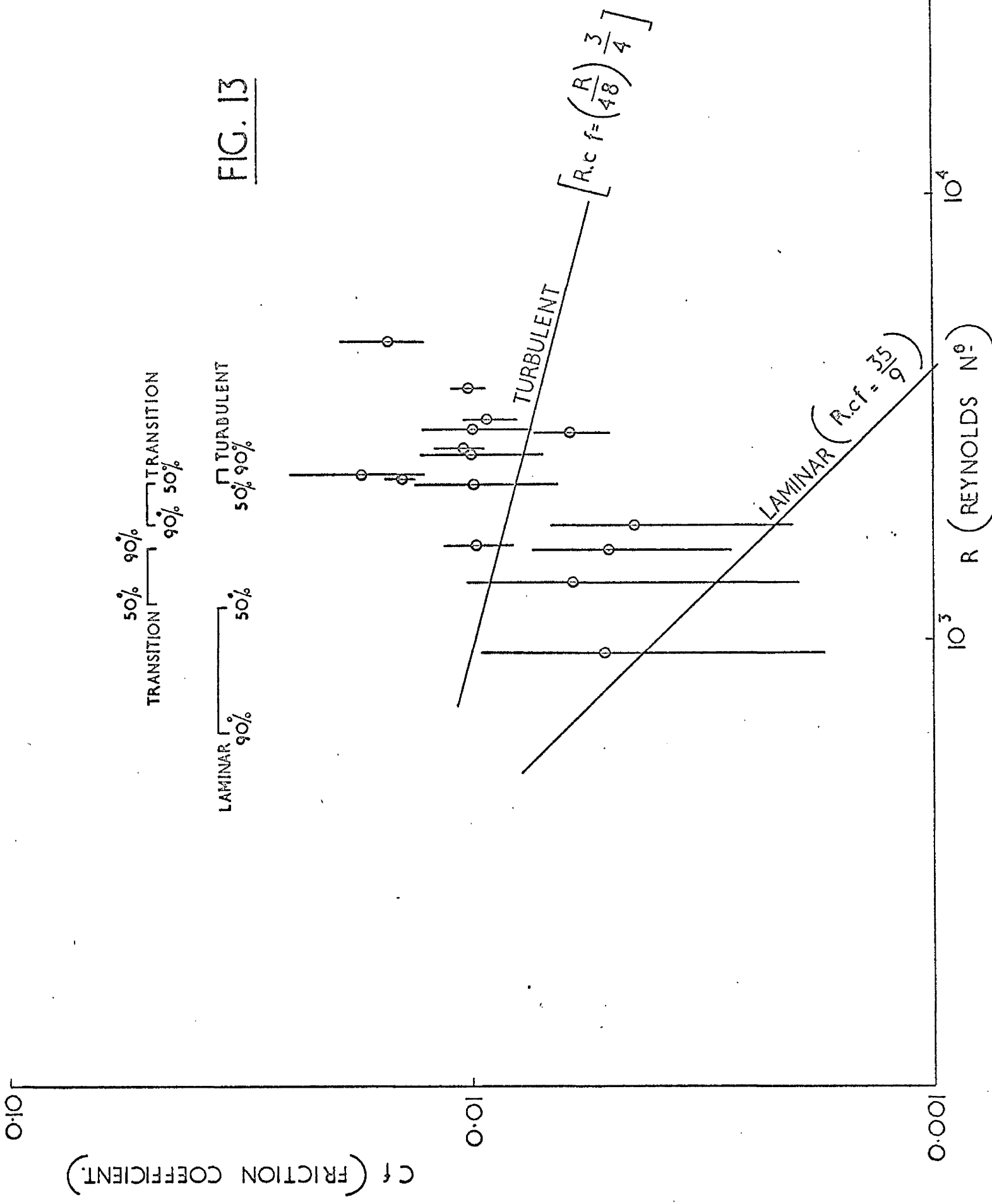


FIG. 12

FIG. 13



GLASGOW
UNIVERSITY